universität wien

MASTERARBEIT | MASTER'S THESIS

Titel | Title

Analysis of Wnt4EMS23 in the remodelling of AB neurons

verfasst von | submitted by

Mariam Kassem BSc

angestrebter akademischer Grad | in partial fulfilment of the requirements for the degree of

Master of Science (MSc)

Wien | Vienna, 2025

Studienkennzahl lt. Studienblatt | Degree programme code as it appears on the student record sheet:	UA 066 878
Studienrichtung lt. Studienblatt | Degree programme as it appears on the student record sheet:	Masterstudium Verhaltens-, Neuro- und Kognitionsbiologie
Betreut von | Supervisor:	Univ.-Prof. Dr. Thomas Hummel

Table of Contents

Acknowledgements

I would like to express my deepest gratitude to all those who have supported and contributed to the completion of this thesis.

First and foremost, I would like to thank my unofficial supervisor, Johann Markovitsch, for his invaluable guidance, encouragement, and expertise throughout the course of my research. His constant support and insightful feedback have been crucial to the development of this work.

I also wish to acknowledge my supervisor and professor Thomas Hummel, whose assistance and advice have significantly enhanced my research. I am grateful for the time and effort he dedicated to helping me refine my ideas and approach.

I would like to express my sincere gratitude to my colleagues and fellow researchers in the Hummel lab, whose collaborative attitude and insightful discussions not only enhanced my research but also brought me great joy. A special thanks to Orkun, Aygül, Aron, and Elif, my fellow master's students, for their friendship and support throughout this journey. I would also like to thank Wolfgang, Sigi, Alex, Huey, Daniel, and Alisa for making lunch breaks an enjoyable part of my day.

Finally, I am deeply grateful to my parents for their unwavering support and encouragement, my siblings for the scientific discussions and encouragement throughout this journey as well as the support of my best friend, Iman, who kept reminding me not to stress myself. Their belief in me has been a constant source of motivation.

Thank you all for your contributions, which have made this thesis possible.

Abstract

Neuronal remodelling during development involves changes in the structure and connectivity of neurons as the brain matures. This includes the dynamic formation of new synapses, the refinement of existing ones, and the elimination of inactive connections, the brain's circuitry to enable efficient communication and facilitate cognitive and motor skills development. How molecular programs control the precise neuronal remodelling is poorly understood. In Drosophila melanogaster, commissural SA^{uni} neurons in the central brain undergo unilateral pruning to build a bilaterally asymmetric circuit organization. A mutation in the conserved wingless pathway component Wnt4 (*wnt4*^{EMS23}) disrupts SA^{uni} lateralization, while a defined *wnt4* loss-of-function allele does not interfere with the remodelling process. By testing for genetic interaction of *wnt4*^{EMS23} with other components of the Canonical Wnt Signalling Pathway, the mutant's function was determined. The results show that *wnt4*^{EMS23} acts as a gain-of-function mutant, indicating enhanced Wnt4 signalling with the addition of enhanced release of Armadillo, and that Arrow, a co-receptor to frizzled, plays a crucial role in neuronal remodelling. Additionally, the APC protein, which regulates the Wnt pathway and maintains cellular stability, contributes to the remodelling process. These interactions between *wnt4*^{EMS23}, Armadillo, Arrow, and APC are vital for the structural changes necessary for proper lateralization of neuronal development.

Zusammenfassung (Deutsch)

Die neuronale Umstrukturierung während der Entwicklung umfasst Veränderungen in der Struktur und Konnektivität von Neuronen, während das Gehirn heranreift. Dazu gehören die dynamische Bildung neuer Synapsen, die Verfeinerung bestehender Verbindungen und die Eliminierung inaktiver Synapsen, wodurch die Schaltkreise des Gehirns effizientere Kommunikation ermöglichen und die Entwicklung kognitiver und motorischer Fähigkeiten fördern. Wie molekulare Programme diese präzise neuronale Umstrukturierung steuern, ist bislang nur unzureichend verstanden. Bei *Drosophila melanogaster* unterziehen sich die kommissuralen SA^{uni}-Neuronen im Zentralgehirn einer einseitigen Pruning-Phase, um eine bilateral asymmetrische Schaltkreisorganisation aufzubauen. Eine Mutation in der konservierten Wingless-Signalweg-Komponente Wnt4 ($wnt4^{EMS23}$) stört die Lateralisation der SA^{uni}-Neuronen, während ein definierter *wnt4*-Loss-of-Function-Allel den Umstrukturierungsprozess nicht beeinträchtigt. Durch das Testen genetischer Interaktionen zwischen $wnt4^{EMS23}$ und anderen Komponenten des kanonischen Wnt-Signalwegs konnte die Funktion der Mutante bestimmt werden. Die Ergebnisse zeigen, dass $wnt4^{EMS23}$ als Gain-of-Function-Mutante wirkt, was auf eine verstärkte Wnt4-Signalisierung hinweist, einschließlich einer erhöhten Freisetzung von Armadillo. Zudem spielt Arrow, ein Korezeptor von Frizzled, eine entscheidende Rolle in der neuronalen Umstrukturierung. Zusätzlich trägt das APC-Protein, das den Wnt-Signalweg reguliert und die zelluläre Stabilität aufrechterhält, zum Remodelling-Prozess bei. Diese Interaktionen zwischen $wnt4^{EMS23}$, Armadillo, Arrow und APC sind essenziell für die strukturellen Veränderungen, die für eine korrekte Lateralisation der neuronalen Entwicklung erforderlich sind.

1. Introduction

1.1 Asymmetric Bilateria

Most animals are considered bilaterally symmetric. In fact, most metazoans, which make up the Bilateria, are named for their bilateral body symmetry. This symmetry arises from the intersection of two orthogonal axes: the anterior-posterior axis and the dorsal-ventral axis (Finnerty 2003). While this assertion appears accurate at first, a deeper examination reveals that these animals may be more asymmetrical than previously thought.

Externally, humans may appear symmetrical, yet internally, asymmetries are common. For instance, the spleen is located only on the left side, and the left lung has two lobes, while the right lung has three. Additionally, both our heart and stomach are positioned to the left of the body's central axis. This asymmetry extends beyond anatomy to behaviour as well; approximately one in ten people are left-handed instead of right-handed. This preference for one hand over the other highlights the asymmetry in our behaviour (Held, 2009).

Lateralization in the brain refers to the functional dominance of one side over the other (Noggle and Hall, 2011). The two hemispheres process information differently and govern distinct patterns of behaviour (Rogers, 2021). The left hemisphere is recognized for having a higher concentration of grey matter and greater cell density, featuring more non-myelinated fibres and specialized areas for motor and specific sensory functions. In contrast, the right hemisphere is characterized by a greater number of myelinated axons that connect different brain regions (Brownell et al., 2000). Altered hemispheric asymmetry is linked to various mental illnesses, including Alzheimer's, ADHD, autism, psychotic disorders, and others (Kong et al., 2022). Thus, these asymmetries play a crucial role in maintaining a healthy brain.

These asymmetries are observed not only in humans but also in other metazoans, many of which are being studied for their asymmetrical traits. One well-known model organism is the zebrafish, or *Danio rerio*. This tropical freshwater fish exhibits significant asymmetry in its epithalamus, which can be genetically modified to track the development of structural asymmetries. The epithalamus includes a portion of the

diencephalon and the habenula, which connects the forebrain to the ventral brain (Güntürkün and Ocklenburg, 2017). Another model organism studied for brain asymmetry is the fruit fly, or *Drosophila melanogaster*.

Although the majority of the neuropils in the central complex are symmetrical, the complex contains a bilateral structure called the asymmetric body (AB) (Scheffer et al., 2020). The AB is a pair of synaptic neuropils with interacting axons, dendrites, and glial cells (Hirase and Shinohara, 2014), on each side of the midline, which differ in size (Wolff and Rubin, 2018). This area plays a crucial role in spatial control and motor activity (Lapraz, 2023). It appears that asymmetries are a general concept in nature, not limited to just vertebrates (Güntürkün and Ocklenburg, 2017).

1.2 Asymmetric body in *Drosophila melanogaster*

To further investigate the development of the brain asymmetry, the fruit fly, *Drosophila melanogaster,* serves as an excellent model organism. It has been used in research for over a century due to its cost-effectiveness and rapid generation time. Additionally, the availability of advanced genetic tools has made the fruit fly indispensable in scientific studies, with an increasing number of molecular techniques being developed, enhancing its value as a model organism (Tolwinski, 2017).

The left-right structure of the asymmetric body (AB) of *Drosophila melanogaster* was first described in 2004 (Pascual et al., 2004). The AB is situated within the central complex, which also includes the fan-shaped body (FB), protocerebral bridge (PB), ellipsoid body (EB), and noduli (NO). Researchers observed that the AB, a neuropil, is located at the midline, in front of the ventral FB (Wolff and Rubin, 2018).

The majority of wild-type flies show a right-directed bilateral asymmetric body, with the neuropil being larger in the right hemisphere compared to the left. The AB consists of three cell types, two of which exhibit a unilateral phenotypic pattern (Wolf and Rubin, 2018). The SA^{uni} -neurons display a unilateral phenotype, while the Sa^{bi}-neurons show a bilateral phenotype. Approximately 10% of brains exhibit a bilateral phenotype, contrasting with the more common unilateral phenotype of the AB. SA^{uni}- neurons express Fasciclin II (Fas II) (Coutelis et al., 2008). Fas II is a cell-adhesion molecule that

regulates motoneuron innervation of muscle fibers (Turrigiona, 1999). This allows researchers to stain brains with an anti-Fas II antibody, making the expression of the unilateral neuron types of the AB visible.

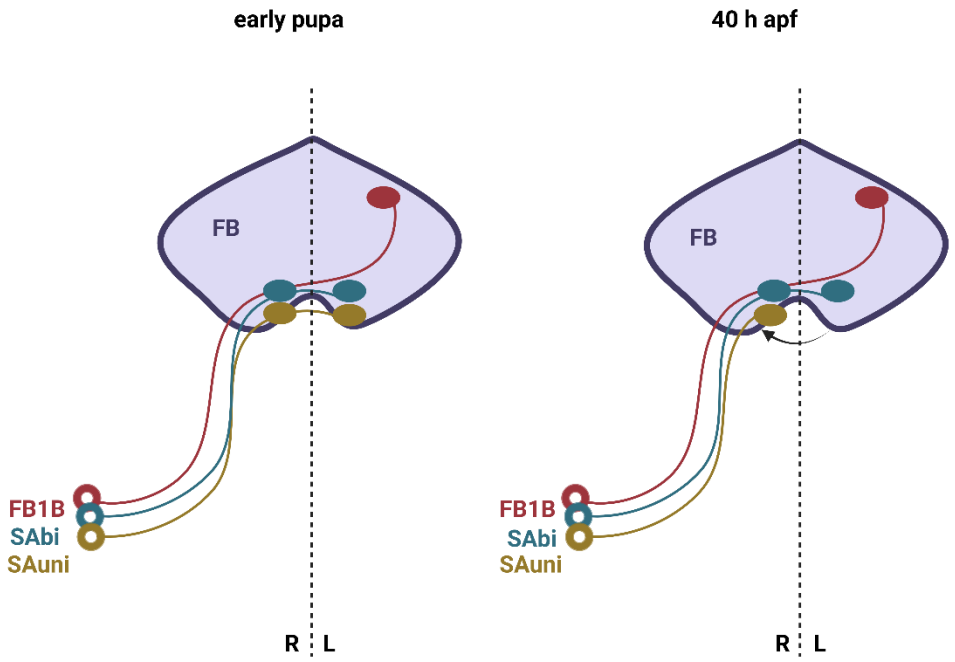

Figure 1: Remodelling of the SAuni neurons: FB1B are neurons of the Fan-shaped body (FB). SAuni and SAbi are distinct cell types of the Asymmetric body (AB). At 40 hours after puparium formation (apf), the left neuropil of SAuni neurons has already retracted to the right side, resulting in a unilateral phenotype. Created in https://BioRender.com

In 2014, it was suggested that the development of unilateral innervation of the AB occurs during morphogenesis (Géminard et al., 2014), a concept that was later further investigated by the Hummel lab. Their research revealed that the AB consists of distinct groups of neurons, namely the SA^{uni} and SA^{bi}. During the early pupal stage, both exhibit a bilateral innervation in the AB (Fig.1). However, during metamorphosis, the SA^{uni} undergoes remodelling and shifts to one side, a process that appears to occur around the 30-hour APF (after pupa formation) (Johann Markovitsch, Msc thesis, 2019).

1.3 Wnt4 shows involvement in remodelling of SA^{uni} neurons

Following the discovery of AB remodelling, the Hummel lab began investigating potential pathways involved, including those related to Wnt molecules. Wnt proteins are involved

in 3 main pathways, the Canonical Wnt-Pathway, the Non-Canonical Planar Cell Polarity Pathway and the Non-Canonical Wnt/Ca^{2+} Pathway (Komiya and Habas, 2008) (Fig.2).

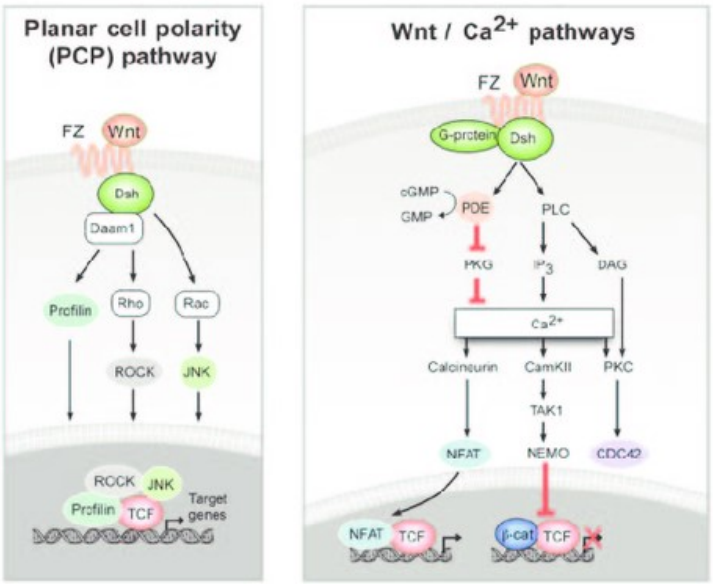

Figure 2: Two of the main Wnt Pathways. The PCP pathway (left) involves activation of small GTPases (Rho, Rac) via Dishevelled (Dsh), affecting cytoskeletal dynamics and gene transcription. The Wnt/Ca^{2+} pathway (right) triggers intracellular calcium release through G-protein signalling, leading to activation of effectors like PKC, CamKII, and calcineurin, ultimately influencing transcription factors such as NFAT and TCF (Figure from: Le Bras et al., 2010).

The Non-Canonical Planar Cell Polarity Pathway is divided into three Pathways (Fig.2). Wnt signalling activates Dishevelled (Dsh) through Frizzled (Fz) receptors, independent of the co-receptor Arrow. Dsh then triggers multiple pathways. **Rho Activation**: Dsh activates Rho via Daam1, leading to Rho kinase (ROCK) activation, **Actin Polymerization**: Daam1 also promotes actin polymerization through Profilin and **Rac Activation**: Dsh activates Rac, which in turn activates JNK. These pathways (ROCK, JNK, and Profilin) are known to work together to coordinate cytoskeletal changes essential for cell polarization and motility during gastrulation (Komiya and Habas, 2008).

The Non-Canonical Wnt/Ca^{2+} Pathway also follows multiple pathways once activated (Fig.2). Wnt signalling through Fz activates Dsh via G-proteins. Dsh triggers several pathways. First **PDE Activation**: Dsh activates PDE, inhibiting PKG and reducing Ca2+ release, secondly **IP3 and Ca2+ Release**: Dsh activates PLC, producing IP3, which releases intracellular Ca2+, activating CamK11 and calcineurin. Calcineurin activates NF-AT to regulate ventral cell fates. CamK11 activates TAK and NLK, inhibiting β-catenin/TCF to control dorsal axis formation. Lastly **DAG/PKC/CDC42 Pathway**: DAG

activates PKC, which activates CDC42, driving tissue separation and cell movements during gastrulation. These signalling events coordinate cell fate determination and morphogenetic movements during development (Komiya and Habas,2008).

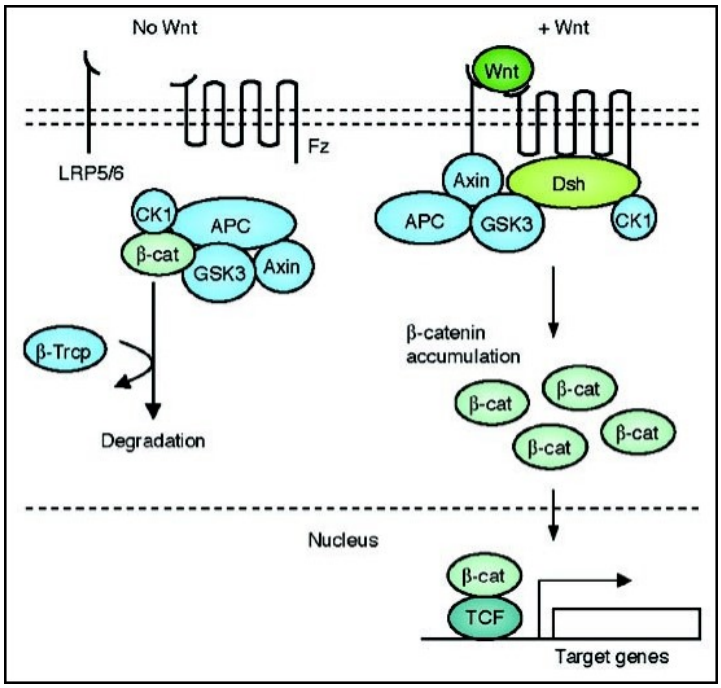

Figure 3: The Canonical Wnt-Signalling Pathway. When activated, a cascade of events occurs, leading to the release of ß-catenin, which subsequently promotes the expression of target genes. In the absence of Wnt, ß-catenin is phosphorylated by the Axin complex and is then degraded (Komiya and Habas, 2008).

The Canonical Wnt-Pathway is also known as the Wnt/ β -catenin Pathway (Fig.3). In the **absence of Wnt**, the destruction complex, consisting of Axin, APC, GSK3-β, and CK1, remains active and promotes the degradation of β-catenin (known as Armadillo in *Drosophila melanogaster*). CK1 and GSK3-β phosphorylate Armadillo, creating a binding site for the ligase β-TrCP, which then facilitates its degradation. In contrast, when **Wnt is present**, it binds to a Frizzled receptor and a co-receptor complex, leading to the recruitment of Disheveled (Dsh) to the cell membrane. The co-receptor becomes phosphorylated and binds to Axin, removing it from the destruction complex. This disassembles the complex and releases Armadillo, which is then transported to the nucleus. There, Armadillo binds to the transcription factor TCF, initiating gene expression (Qin et al., 2023).

In Drosophila, four Frizzled receptors have been identified: Fz, Fz2 (Graba et al., 2000-2013), Fz3 (Sun et al., 2023), and Fz4 (McElwain et al., 2011). Additionally, three co-receptors play a key role: Arrow (also known as LRP5/6, Graba et al., 2000-2013), and

two Drosophila Ror homologs, Ror and Neurospecific receptor kinase (Nrk) (Ripp et al., 2018).

Wnt4 signalling in the Drosophila brain has been shown to regulate various aspects of neuronal development, including neurogenesis, axon guidance, and synaptic function (Wu et al.,2013). In the vertebrate cerebellum, Wnt signalling operates as a retrograde cue originating from granule cells, promoting presynaptic differentiation of mossy fibres and functioning as a key synaptogenic factor (Rosso and Inestrosa, 2013). Wnt4 is involved in establishing the proper patterning of cells through long range directional signalling. It helps ensure the correct differentiation of neural cells in specific regions of the developing nervous system (Wu et al., 2013).

As mentioned, Wnt4 plays a significant role in the directional guidance of axons during neural development. It acts through the Wnt signalling pathway, where it interacts with receptors on the growth cones of axons, influencing their movement toward specific targets. It contributes to establishing axonal polarity and ensuring correct axon pathfinding to form functional neural circuits. Thus, Wnt4 provides essential signalling cues that help neurons navigate their environment and form accurate connections within the developing nervous system (Schnorrer and Dickson, 2004).

Lastly, Wnt4 is shown to play a key role in synapse formation and the development of neuronal circuits. It regulates the assembly of presynaptic and postsynaptic sites, facilitating effective neuron communication. Furthermore, it helps refine and stabilize neural connections, ensuring proper neuronal circuit wiring and communication, which are crucial for behaviour and cognitive function (Park and Shen, 2012).

Wnt4 was identified as a candidate gene in a screen of RNAi knockdowns and mutant fly lines for asymmetric development of the AB. They showed a significantly increased rate of bilateral asymmetric bodies (AB) in the brain.

Subsequently, they tested two Wnt4 mutants, $wnt4^{C1}$ and $wnt4^{EMS23}$, to assess whether any effect on AB could be observed (Fig. 4). Although both mutants are described as a Loss-of-function mutant, only $wnt4^{EMS23}$ exhibited a significant difference compared to the wild-type fly, posing a question of its real function.

Developmental temperature changes also influenced the mutations impact on bilateral innervation of SA^{uni}. At 18°C, *wnt4*^{EMS23} demonstrated over 90% bilateral SA^{uni} phenotypes, whereas the wildtype flies showed only about 10% bilaterality. At 25°C, the bilaterality effect decreased, but it remained notably higher than that of the control (Johann Markovitsch, unpublished).

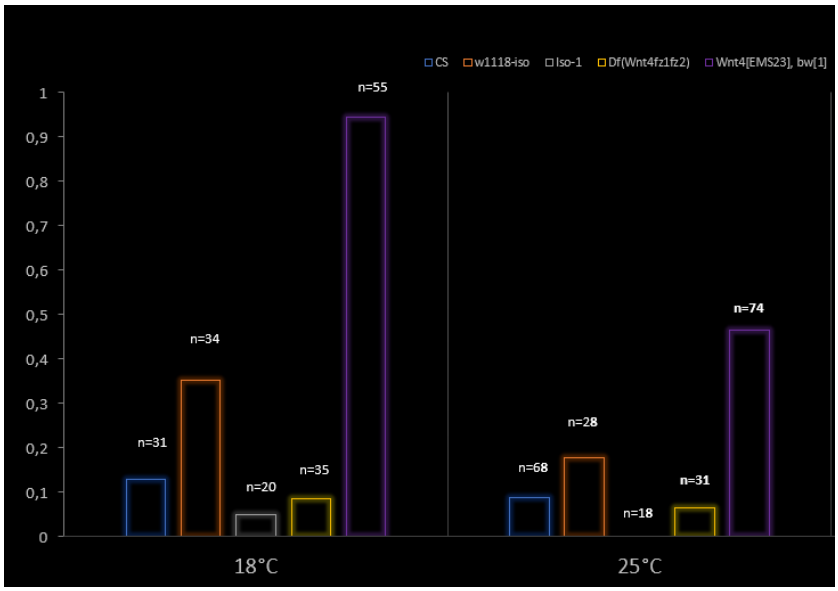

Figure 4: *Ratio of bilateral Phenotypes of SA^{uni} at two experimental temperatures for different Wnt4 related lines. Wnt4^{Ems23} show an increase bilaterality rate compared to the other lines at both temperatures. CS = Canton S, ^{w1118}-iso = isogenised wildtype (most common genetic background), Iso-1 = isogenised wildtype, Df(Wnt4fz1fz2) = Wnt4^{Ems23} with fz1^{R52} hypomorph and fz2 deletion, Wnt4(EMS23) = wnt4 mutant. Made by Johann Markovitsch*

This led the lab to investigate the strength of the mutation. To do so, they crossed the mutant flies to wildtype flies, until only a heterozygous copy of *wnt4*^{EMS23} was present. To eliminate the influence of genetic background on the bilateral phenotype, the stocks were isolated by crossing the mutant lines with different Balancer lines. For instance, the wnt4 mutant (; $\frac{wnt4^{EMS23},bw^{1}}{Cyo}$;) was crossed with a Balancer line (; ; $\frac{TM3}{TM6}$). After six successive crosses with the same Balancer stock, approximately 99% ($1 - 0{,}5^{6} = 0{,}98$) of the genetic background was derived from the Balancer stock. This process was repeated for each chromosome until the majority of the genetic background was removed. The isolated stock showed a reduced rate of bilateral phenotypes. The rate dropped to around 45% *(Johann Markovitsch, unpublished)*.

1.4 Aim of Thesis

This thesis explores the effect of *wnt4*^{EMS23} mutation on AB remodelling. Its goal is to determine whether the mutant truly represents a loss-of-function mutation for Wnt4 as described or rather a causing a constant activation of Wnt4. This will be determined by calculating the percentage of bilateral AB phenotypes of SA^{uni}-neurons. My investigation will focus on key components of the Canonical Wnt Signalling Pathway (Fig. 3).

The experiments will focus on key components of the pathway, including the receptors, co-receptors, Armadillo, and APC.

I hypothesize that an active Canonical Wnt-Signalling Pathway disrupts the initiation of the remodelling in SA^{uni} neurons, resulting in a bilateral phenotype. To test this, I will knock down various components of the pathway in Frizzled-expressing cells and those connected to the Asymmetric Body. My objective is to develop a model that contributes to understanding the remodelling process of SA^{uni} neurons.

If the mutant is a gain-of-function, then the presence of the activated form of Armadillo, which would promote an active Wnt pathway, should increase the rate of bilaterality in the asymmetric body. If the statement proves true, it will indicate that the Canonical Wnt Signalling Pathway indeed plays a role in the remodelling process of the asymmetric body in SA^{uni} neurons.

2. Material and Methods

2.1 Material

2.1.1 Fly constructs

Experimental Drosophila melanogaster constructs were maintained at 25 °C, standard lab conditions, or at 18 °C. An overview of the fly constructs used in this project and their sources is provided in Table 1. A total of 7 Gal4-lines were utilized in my experiments, of which 3 are directly linked to the Asymmetric body (AB) and 4 are associated with Wnt molecules.

To visualize the expression patterns of the various Frizzled receptors, 10x UAS-mCD8::GFP was coupled with the respective Gal4 lines. To determine whether the Canonical Wnt-Signalling Pathway influences the bilateral phenotype of the SAuni neurons, I employed both a constitutively active form of Armadillo, also known as β-catenin, and a knockdown of it, using the mentioned Gal4 lines. Another approach I used to investigate the potential involvement of this pathway in remodelling was the knockdown of APC in AB-involved or Frizzled-expressing cells. For some of the Gal4 experiments, I labelled SA^{uni} neurons with a marker, produced by meiotic recombination of R72A10-lexA and 10xlexaAop-mCD8::GFP. Finally, various mutants were tested; *wnt4*^{EMS23} was coupled with both UAS-Armadillo and crossed with the Gal4 lines. The other mutants used were null alleles (*Nrk*^{KO}, *fz4*$^{3-1}$, *Ror*^{4}, *arr*^{2}).

Table 1: *Fly Constructs*

Name	Source	Reference
Fz-Gal4	Bloomington Drosophila Stock Center	Bellen et al., 2011
Fz2-Gal4	Bloomington Drosophila Stock Center	Bellen et al., 2011
Fz3-Gal4	Bloomington Drosophila Stock Center	Sivasankaran et al., 2000
Fz4-Gal4	Bloomington Drosophila Stock Center	Kanca et al., 2022

R72A10-Gal4	Bloomington Drosophila Stock Center	Jenett et al., 2012
R66A02-Gal4	Bloomington Drosophila Stock Center	Jenett et al., 2012
R16E08-Gal4	Bloomington Drosophila Stock Center	Jenett et al., 2012
UAS-arm^{RNAi}	Bloomington Drosophila Stock Center	Perkins et al., 2015
UAS-arm^{act}	Bloomington Drosophila Stock Center	Pai et al., 1997
UAS-APC^{RNAi}	Vienna Drosophila Resource Center	Dietzel et al., 2007
10x UAS-mCD8::GFP	Bloomington Drosophila Stock Center	Hadjieconomou et al., 2011
Wnt4^{EMS23}	Not known	
Nrk^{KO}	Bloomington Drosophila Stock Center	Fradkin, L., 2023
Ror^{4}	Bloomington Drosophila Stock Center	Ripp et al., 2018
arr^{2}	Bloomington Drosophila Stock Center	Tearle, R.G., Nusslein-Volhard, C., 1987
Fz4$^{3-1}$	Bloomington Drosophila Stock Center	McElwain et al., 2011
R72A10-lexA	Bloomington Drosophila Stock Center	Jenett et al., 2012
10x lexAop-mCD8::GFP	Bloomington Drosophila Stock Center	Hadjieconomou et al., 2011

2.2 Methods

2.2.1 Binary Expression Systems

Almost all the experiments utilize binary expression systems (Gal4/UAS, LexA/LexAop). This system consists of two constructs: one drives the expression of the gene encoding Gal4 through a cell-specific promoter, while the second construct uses the UAS (upstream activation sequence) to regulate the desired transgene. The GAL4 complex binds to the UAS sequence, facilitating the expression, knockdown, or activation of the gene. As a result, only the cells regulated by the Gal4 promoter will express the transgene (Carter and Shieh, 2015). The LexA/LexAop expression system works the same way.

2.2.3 RNAi Knock Down

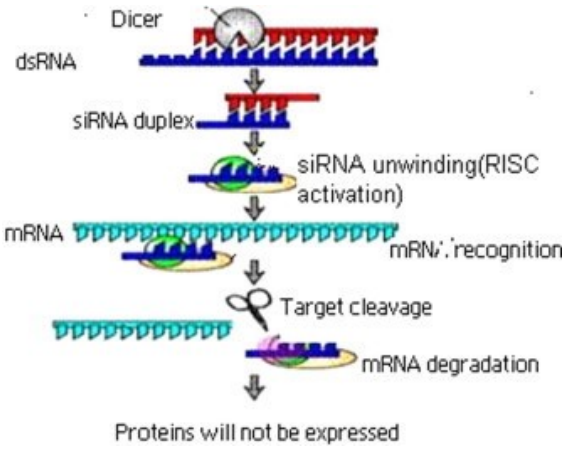

Figure 5: *Mechanism of RNAi (Ambesajir et al., 2012)*

RNA interference (RNAi) is a mechanism for regulating gene expression (see Fig. 5). Double-stranded RNA (dsRNA) inhibits the production of its target protein. This dsRNA is processed into short interfering RNAs (siRNAs) by the endonuclease Dicer. These siRNAs are then incorporated into the RNA-induced silencing complex (RISC). The helicase within RISC unwinds the siRNA, allowing it to bind to complementary antisense mRNA strands. This interaction leads to the cleavage of the mRNA, preventing it from proceeding to translation (Ambesajir et al., 2012). Researchers have developed a

method to achieve targeted knockdown in specific cells by integrating this system with the GAL4/UAS binary system (Dietzl et al., 2007). In my project, I applied this approach to knock down both Armadillo and APC.

2.2.4 Constantly active gene

In my project, I utilized a continuously active form of Armadillo, which was developed by Pai and his colleagues through the deletion of 54 amino acids from the N-terminal domain using an in vitro mutagenesis kit. The deleted regions include the GSK/Zw3 phosphorylation site, which, together with APC, leads to the degradation of Armadillo, as well as a binding site for cactus, the fly homolog of IκB (Pai et al., 1997), which regulates ubiquitination IκB (Bergmann et al., 1996).

2.2.5 Immunohistochemistry

To visualize the expression of various proteins, I employed immunohistochemistry (IHC), specifically using an indirect IHC approach to amplify the signal. This method allows multiple secondary antibodies to bind to a single primary antibody. It's important that the two antibodies are produced in different species, and the secondary antibody must be directed against the correct immunoglobulin molecule of the primary antibody (Carter and Shieh, 2015).

Drosophila melanogaster flies were dissected when they were 3 to 5 days old, or during the pupal stage at approximately 30 to 50 hours after pupa formation. The **dissections** were carried out in phosphate-buffered saline (PBS). After extracting the brains, they were **fixed** in a 4% paraformaldehyde (PFA) solution in PBS for 30 minutes on a rotator at room temperature. Following fixation, the PFA was removed, and the samples were **washed** 3 to 4 times for 10 minutes each using 0.3% PBT (PBS with Triton X-100) to ensure thorough PFA removal. The samples were then **blocked** with 10% goat serum (diluted in PBT) for about 30 minutes. After blocking, the brains were incubated overnight at 4°C on a shaker with **primary antibodies** (as detailed in Table 2), which were diluted to the appropriate concentration in goat serum. The following day, the tissues were **washed** again 3 to 4 times for 10 minutes in PBT and then incubated overnight at 4°C on

a shaker with **secondary antibodies**. The specific antibodies and their sources are listed in Table 2. On the next day, the samples underwent a **final series of washes** (3 to 4 times for 10 minutes each) and were then ready to be **mounted**. The brains were mounted in Vectashield® (Vector Laboratories) oriented either anterior to posterior or vice versa. To prevent damage to the brains, modelling clay was applied to the corners of the cover slip before placing it on top of the samples. The cover slip was pressed down until the Vector Shield made contact and a bubble formed around the brains. The brains were then ready for imaging.

Table 2: *Antibodies used for staining*

Antibody	Antigene	Origin	Source
Primary	GFP	Rabbit	Invitrogen
Primary	N-cadherin (NCAD)	Rat	Homemade
Primary	Fasciclin 2 (FAS2)	Mouse	Homemade
Secondary	Mouse 488	Goat	Invitrogen
Secondary	Mouse 568	Goat	Invitrogen
Secondary	Rabbit 488	Goat	Invitrogen
Secondary	Rat 647	Goat	Invitrogen

2.2.6 Image acquisition and analysis

Images were captured using a Leica Confocal Microscope TCS SP5II with a 20x objective. Stacks were taken from the ellipsoid body to the end of the fan-shaped body at a spacing of 1.51 µm. The images were collected at a resolution of 512x512 pixels with a speed of 400 Hz. The obtained images were processed using Fiji, an image processing software (Schindelin et al., 2012). The fluorescence levels were adjusted, and the images were rotated and flipped to ensure proper left-right orientation. Statistical analysis was conducted using R (R Core Team, 2021), focusing primarily on the significance of the bilaterality rate, which was assessed using the Chi-squared test.

3. Results

3.1 Wnt4 and Frizzled 3 expression overlaps in a layer of the fan-shaped body

Wnt4 expression was previously investigated by the lab. An expression was shown in the adult and the developing central complex (CX) during time of remodelling (Fig.6). More specifically its expression was present in the noduli and in the fan-shaped body. It showed that Wnt4 is present in the central complex during the critical remodelling step, suggesting Wnt4 could be in some way involved in AB lateralisation, even though there is no expression in the AB. This suggests an indirect role in remodelling (Johann Markovitsch, unpublished).

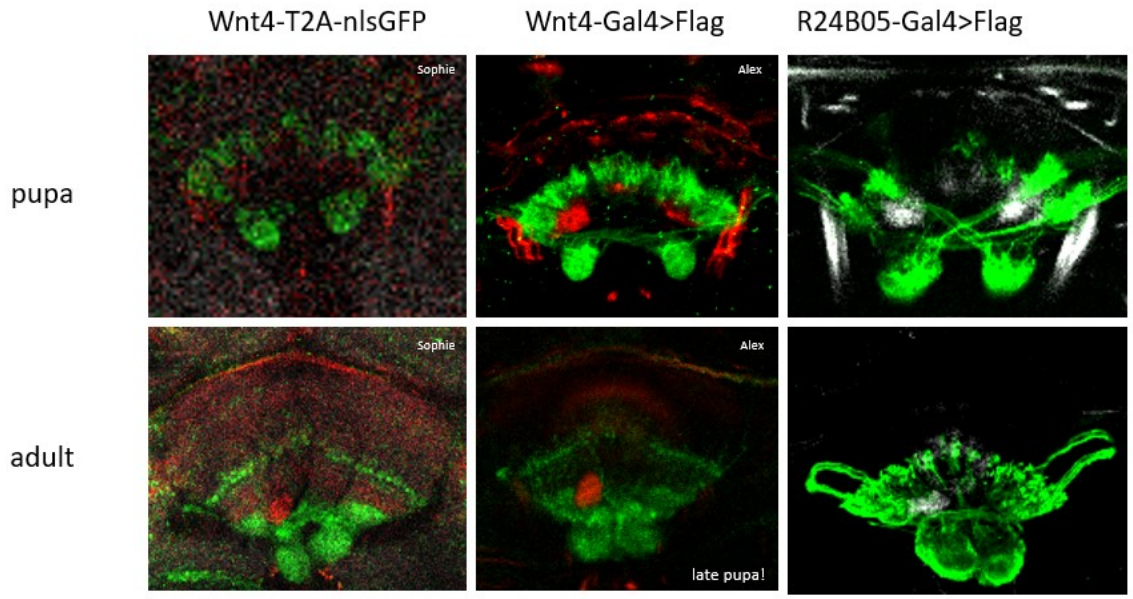

Figure 6: *Expression data of Wnt4 expressing neurons. The upper line of pictures shows Wnt4 expression during the remodelling stag of the AB. The pictures beneath them show the same lines during the adult fly stage. One Wnt4 GFP tagged Drosophila line was used, and two different Wnt4-Gal4 lines were crossed with Flag to show the expression pattern. Wnt4 in green, FasII in red/grey. In green the noduli and part of the fan-shaped body are labelled. In red/grey SA^{uni} neurons are labelled as well as a layer of the fan-shaped body. Made by Johann Markovitsch.*

Since classical Wnt Signalling is mediated by interaction of secreted Wnt4 and transmembrane Frizzled (fz) receptor proteins, I first investigated the distribution of receptors fz1-fz4 in the Drosophila brain and explore their potential role in the remodelling of the asymmetric body (AB). Frizzled Gal4 lines were crossed with UAS reporter lines to visualize the expression (Frizzled 1 (; $\frac{10xUAS-mcD8::GFP}{+}$; $\frac{fz-Gal4}{TM2/TM6B}$),

Frizzled 2 (; $\frac{10xUAS-mcD8::GFP}{+}$; $\frac{fz2-Gal4}{TM2/TM6B}$), Frizzled 3 ($\frac{+}{fz3-Gal4}$; $\frac{10xUAS-mcD8::GFP}{+}$; $\frac{UAS-y}{TM2/TM6B}$), Frizzled 4 ($\frac{+}{fz4-KO-Gal4}$; $\frac{10xUAS-mcD8::GFP}{+}$; $\frac{+}{TM2/TM6B}$)).

Frizzled 1, 2, and 4 exhibit a similar expression pattern in pupal *Drosophila melanogaster* (Fig. 7), mostly observed in the glial cells surrounding the central complex, but not within the neuropiles itself. The pupae examined were between 30 and 40 hours old, a range selected due to the AB remodelling that takes place around 30 hours after pupal formation (APF).

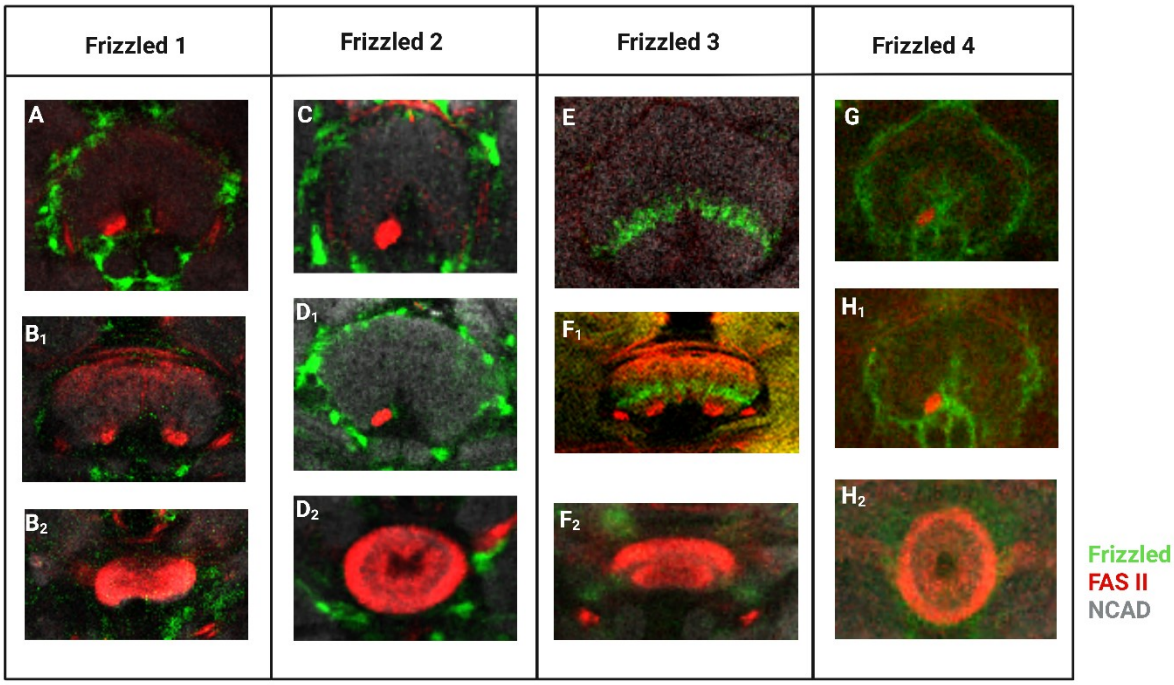

Figure 7: *Different Frizzled Expression Pattern in 30–40-hour pupa. Images A, C, D_1 & D_2, E, G and H_1 & H_2 depict individuals in which AB remodelling has already occurred, suggesting they are older than 40 hours. Images B_1 and B_2 as well as F_1 and F_2 show two individuals in which remodelling has not yet occurred, with B_2 and F_2 highlighting the ellipsoid body. Images D_2 and H_2 display an already formed ellipsoid body. In these images, Frizzled is labelled in green, FAS II in red, and NCAD in grey. Created in https://BioRender.com*

In contrast, Frizzled 3 shows a more distinct expression pattern (Fig. 7). During pupal stage (30-40hrs), Frizzled 3 is expressed in a layer of columnar neurons within the fan-shaped body. Although not shown in the figure, the protocerebral bridge is the only other area of the central complex where Frizzled 3 is found and notably, outside the central complex, the mushroom bodies also exhibit green fluorescence.

Comparing the expression data of Frizzled 1-4 (Fig.7) and Wnt4 (Fig.6) two key overlaps are revealed. First, both Fz3 and Wnt4 are expressed in a layer of the fan-shaped body during both development and in the adult stage. Second, Fz4 expression is observed in the glia above the noduli, which surrounds the expression pattern of Wnt4. Here it is not possible to determine if they coincide, but they are expressed closely to each other.

In summary, there is one certain overlap between the Frizzled 3 receptor and Wnt4. Additionally, Fz, Fz2 and Fz4 are present in the glia in the central complex and Fz3 is present in the fan-shaped body and protocerebral bridge.

The absence of Frizzled receptor expression in the asymmetric body (AB) during the remodelling phase suggests that Frizzled is not directly involved in the remodelling process.

3.3 Canonical Wnt Signalling in AB neurons regulates asymmetric remodelling

Armadillo as well as APC are key components of the Canonical Wnt Signalling Pathway (Fig.3). The potential role of Armadillo in the remodelling of the AB was tested by either activating or knocking it down in AB-associated neurons. Armadillo is typically active when the Canonical Wnt Signalling Pathway is activated, and thus, this experiment aims to determine whether the pathway is involved in the remodelling process.

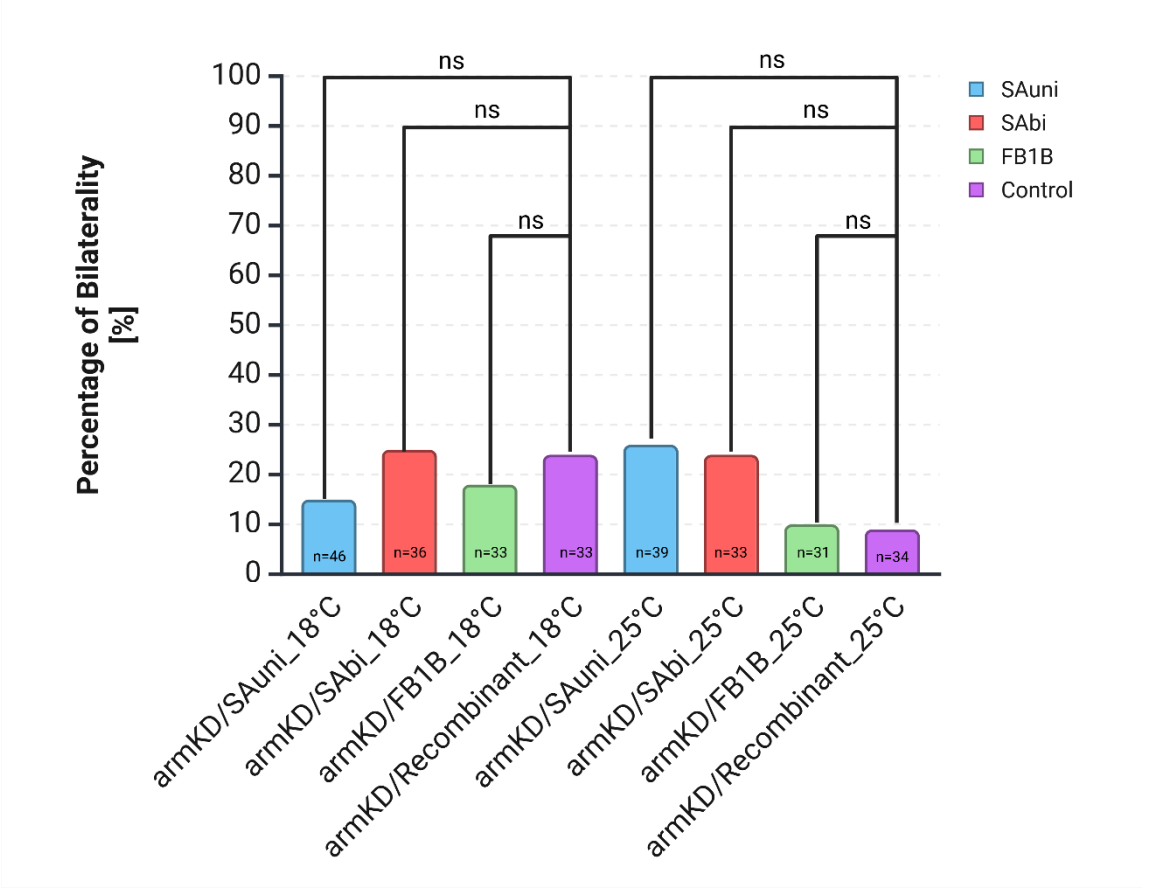

Figure 8: *Armadillo knockdown in AB associated neurons at 18°C and 25°C. Y-Axis shows the percentage of bilateral phenotypes of SA^{uni}. Control being SA^{uni}-GFP-recombinant crossed with the UAS-arm^{RNAi}. No significant effect can be seen. Created in https://BioRender.com*

Armadillo knockdown in SA^{uni} neurons(; $\frac{AB1lexA,lexAop::GFP}{+}$; $\frac{\text{R72A10}-Gal4}{UAS-arm^{RNAi}}$) and SA^{bi} neurons (; $\frac{AB1lexA,lexAop::GFP}{+}$; $\frac{\text{R66A02}-Gal4}{UAS-arm^{RNAi}}$) at 25°C results in a marginal effect on the bilateral innervation of the AB compared to the control (; $\frac{AB1lexA,lexAop::GFP}{+}$; $\frac{+}{UAS-arm^{RNAi}}$) (Fig. 8), without statistical significance.

At this temperature FB1B neurons (; $\frac{AB1lexA,lexAop::GFP}{+}$; $\frac{\text{R16E08}-Gal4}{UAS-arm^{RNAi}}$) show almost the same number of bilateral innervations as the control.

Overall, the percentage of bilateral phenotypes ranges from 15% to 25% across all the knockdowns involving the AB-associated neurons. This suggests that Armadillo has no role in remodelling through these neurons, thus indicating Canonical Wnt Signalling is not involved.

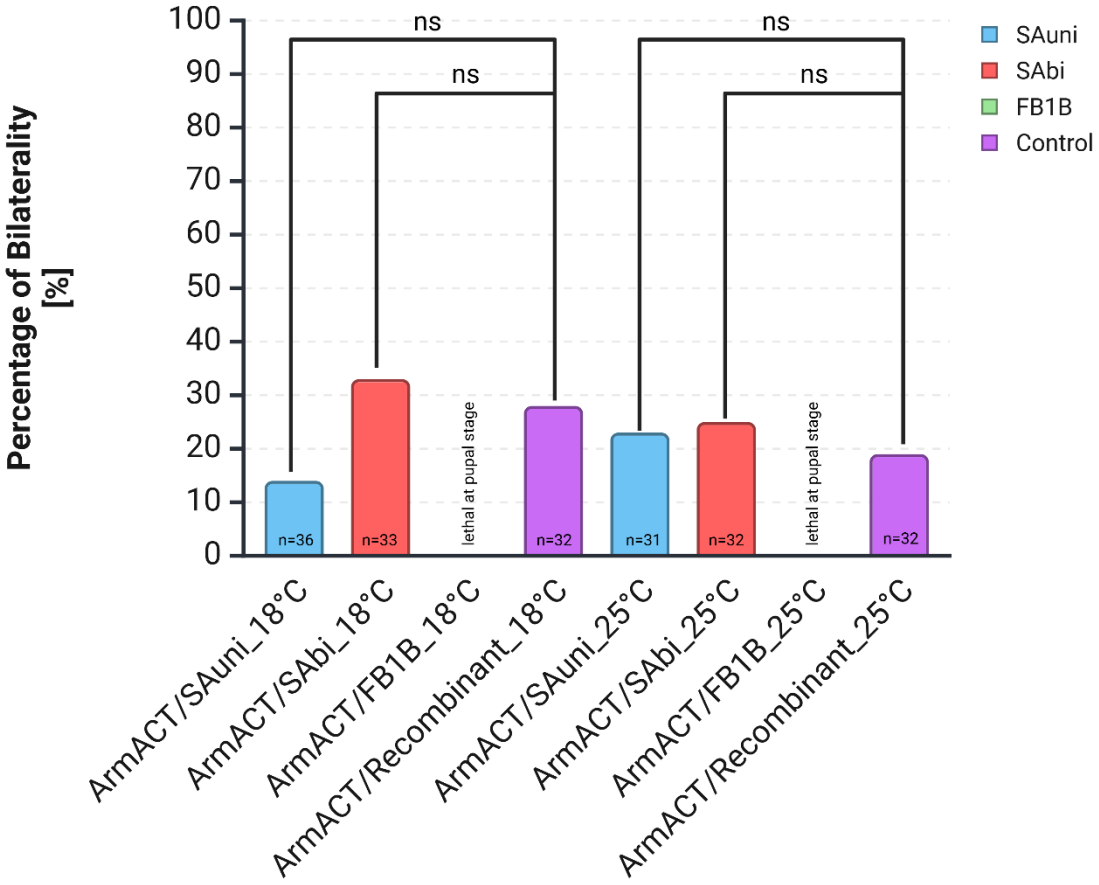

Figure 9: *Armadillo activation in AB associated neurons at 18°C and 25°C. Y-Axis shows the percentage of bilateral phenotypes of SA^{uni}. Control being SA^{uni}-GFP-recombinant crossed with the UAS-arm^{act}. Armadillo activation in FB1B-neurons causes lethality in flies. No significant effect can be seen. Created in https://BioRender.com*

The activation of Armadillo in the same neurons leads to a slightly higher incidence of bilateral phenotypes, ranging from 20 to 25 percent (Fig. 9) at 25°C. No significant difference is observed between the experimental lines SA^{bi} ($\frac{+}{UAS-arm^{act}}; \frac{AB1lexA,lexAop::GFP}{+}; \frac{\mathrm{R66A02}-Gal4}{+}$), SA^{uni} ($\frac{+}{UAS-arm^{act}}; \frac{AB1lexA,lexAop::GFP}{+}; \frac{\mathrm{R72A10}-Gal4}{+}$), and their control ($\frac{+}{UAS-arm^{act}}; \frac{AB1lexA,lexAop::GFP}{+}$;). At 18°C, there is no significant difference, although a slight trend can be observed. SAuni shows a 10% lower frequency compared to its control at the specified temperature. Additionally, it's important to note that crossing FB1B-Gal4 with UAS-arm^{act} leads to complete lethality in the offspring ($\frac{+}{UAS-arm^{act}}; \frac{AB1lexA,lexAop::GFP}{+}; \frac{\mathrm{R16E08}-Gal4}{+}$), preventing the determination of any potential impact on bilaterality.

In summary, the data indicates that Armadillo does not have a significant impact on the remodelling process of SAuni neurons. Despite being a key component of the Canonical Wnt Signalling Pathway, the results suggest that the presence or absence of Armadillo does not appear to affect the structural changes or the transformation of these neurons. Therefore, Armadillo may not play a critical role in the remodelling process of SAuni neurons, at least under the conditions tested in this study.

APC, among other functions, operates in the destruction complex, which degrades Armadillo in the Canonical Wnt Signalling Pathway. Knocking APC down in the same neurons should yield a result like Armadillo activation if it is involved in this pathway.

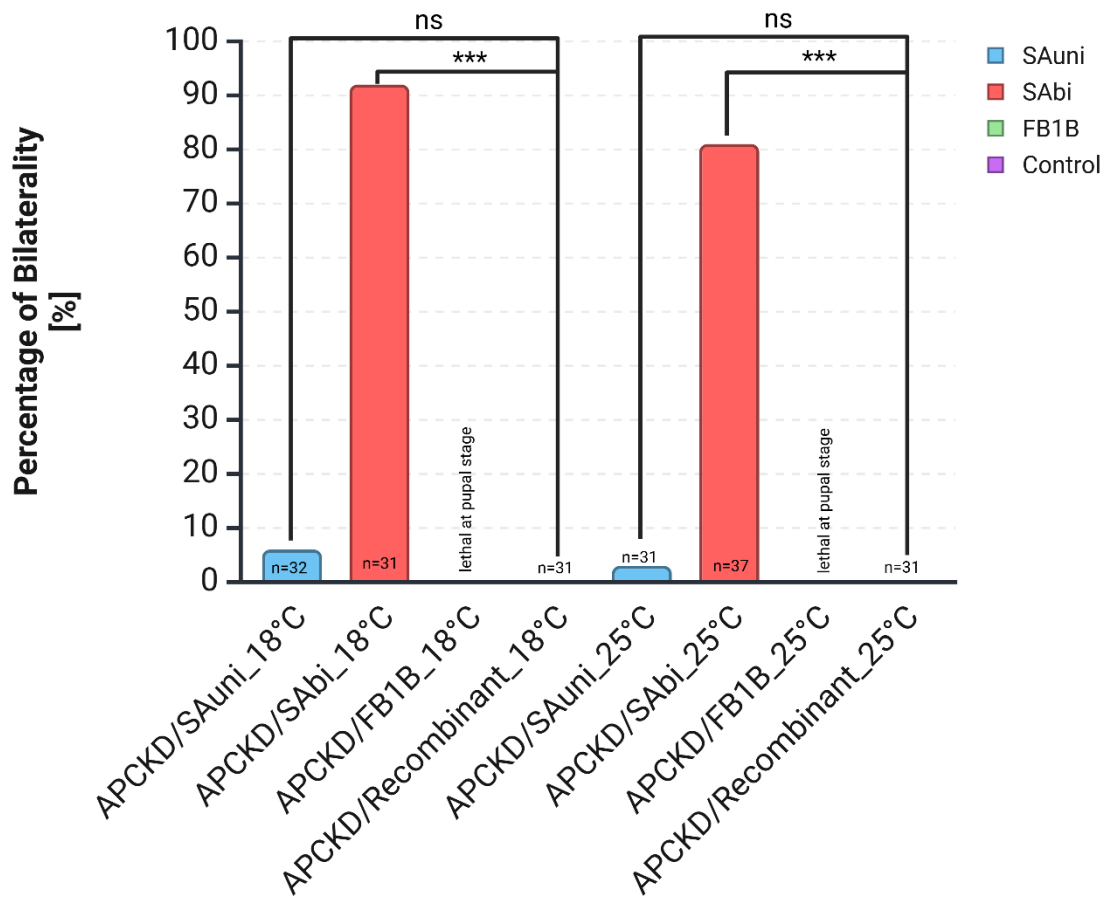

Figure 10: *APC knockdown in AB associated neurons at 18°C and 25°C. Y-Axis shows the percentage of bilateral phenotypes of SA^{uni}. Control being SAuni-GFP-recombinant crossed with the UAS-APC^{RNAi}. APC knockdown in FB1B-neurons causes lethality in flies. Knockdown in SA^{bi}-neurons causes an extremely high bilaterality rate. Created in https://BioRender.com*

RNAi-mediated knock down of APC in the AB-associated neurons (Fig.10):

- SA^{uni} (; $\frac{AB1lexA,lexAop::GFP}{UAS-Apc^{RNAi}}$; $\frac{\mathrm{R72A10-}Gal4}{+}$) shows no significant effect.
- SA^{bi} (; $\frac{AB1lexA,lexAop::GFP}{UAS-Apc^{RNAi}}$; $\frac{\mathrm{R66A02-}Gal4}{+}$), a strong increase of bilateral phenotypes is observed compared to the control (; $\frac{AB1lexA,lexAop::GFP}{UAS-Apc^{RNAi}}$;) at both 18°C and 25°C.

At 18°C, the SA^{bi} crossed offspring exhibit a 90% bilateral phenotype, while the control group shows no bilateral brains (X-squared = 50.792, df = 1, p-value = 1.027e-12, and n = 62). At 25°C, the rate is slightly reduced to 80%, but the difference remains highly significant (X-squared = 41.75, df = 1, p-value = 1.037e-10, and n = 68). Similar to Armadillo activation in FB1B neurons, APC knockdown in these neurons also leads to lethality, making it impossible to assess its role in neuronal remodelling.

These results suggest a strong effect of APC knockdown in SAbi-expressing neurons, leading to a notable and highly significant bilateral phenotype.

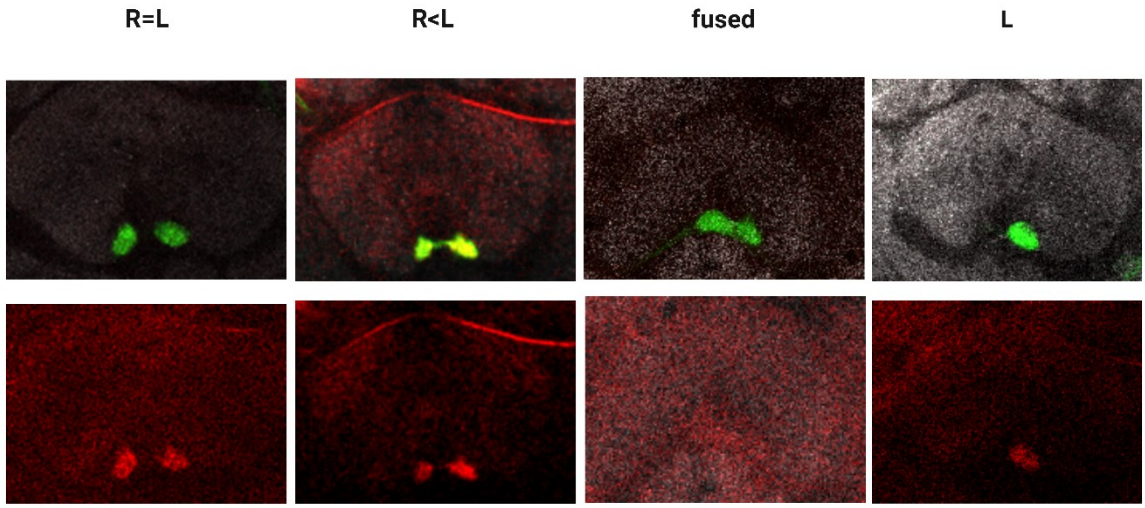

Figure 11: *Unique SA^{uni} neuron Phenotypes when APC is knocked down in SA^{bi} neurons at 18°C and 26°C. GFP in green, FAS II in red and NCAD in grey. The phenotypes are arranged by percentage of occurrence from left to right. FAS II staining in fused example was not good. Created in https://BioRender.com.*

The high frequency of bilateral phenotypes is not the only significant finding when APC is knocked down in SA^{bi} neurons. The SA^{uni} neurons also exhibit distinct phenotypes, which barely appear in the normal development (Fig. 11). Most commonly was the appearance

of same size left-right-AB. In about 10% *of* dissected brains the left AB is larger than the right AB at both temperatures tested. A rarer phenotype is the fused AB, where the commissures between the AB are so thick that they appear fused. Finally, the most distinctive phenotype is the unilateral AB on the left side, instead of the usual right side.

3.3 Frizzled 4 receptor Knockout influences AB remodelling

Armadillos and APCs effect on frizzled expressing cells were tested to determine whether the Canonical Wnt Signalling Pathway is generally involved in AB remodelling.

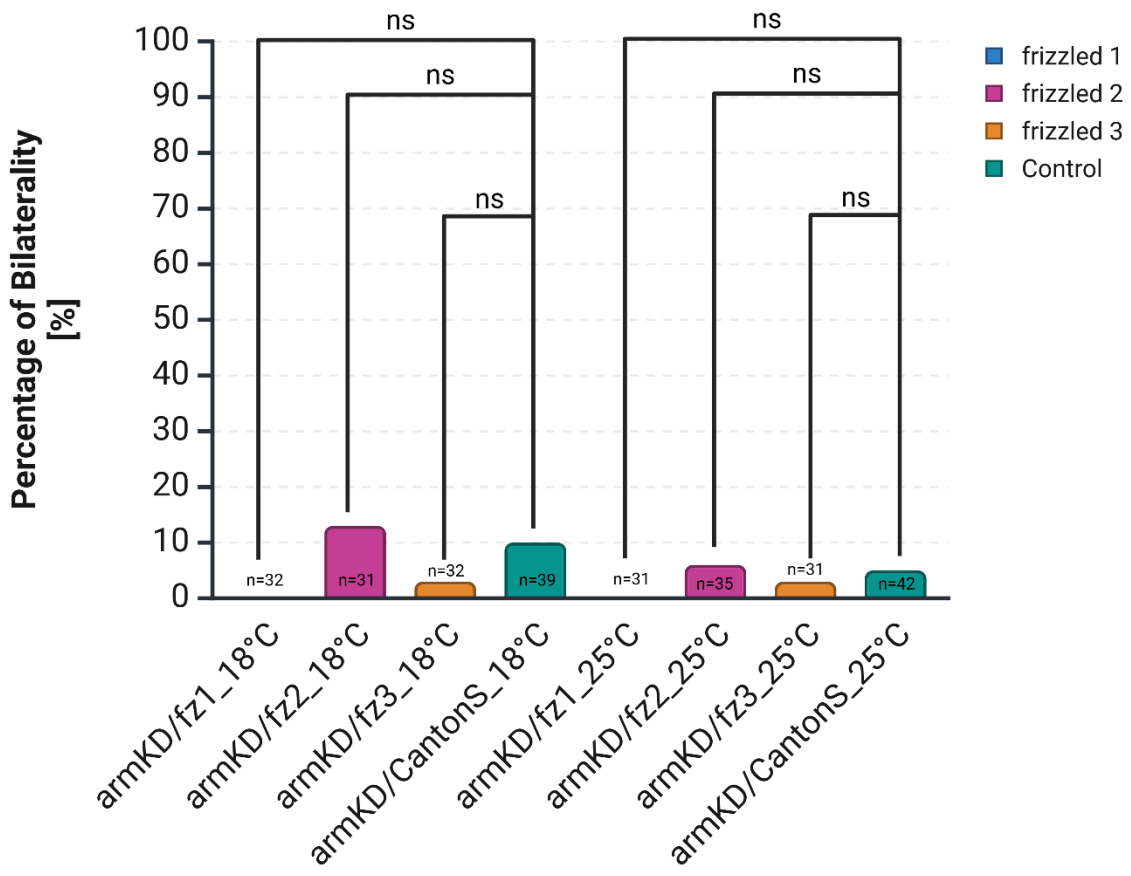

Figure 12: *Armadillo knockdown in Frizzled expressing cells at 18°C and 25°C. Y-Axis shows the percentage of bilateral phenotypes of SA^{uni}. Control being Canton S crossed with the UAS-arm^{RNAi}. No significant effect can be seen. Created in https://BioRender.com*

When Armadillo is knocked down in the Frizzled 1-3 expressing cells ($(;;\frac{fz-Gal4}{UAS-arm^{RNAi}})$, $(;;\frac{fz2-Gal4}{UAS-arm^{RNAi}})$ and $(\frac{+}{fz3-Gal4};;\frac{\mathrm{UAS}-arm^{RNAi}}{UAS-y})$) ,there are little bilateral phenotypes observed (Fig. 12). The controls' $(;;\frac{+}{UAS-arm^{RNAi}})$ bilateral innervations range from 5 to 10

percent at the experimental temperatures. The experimental groups also fall within this range, showing no significant difference between the Frizzled lines and their controls.

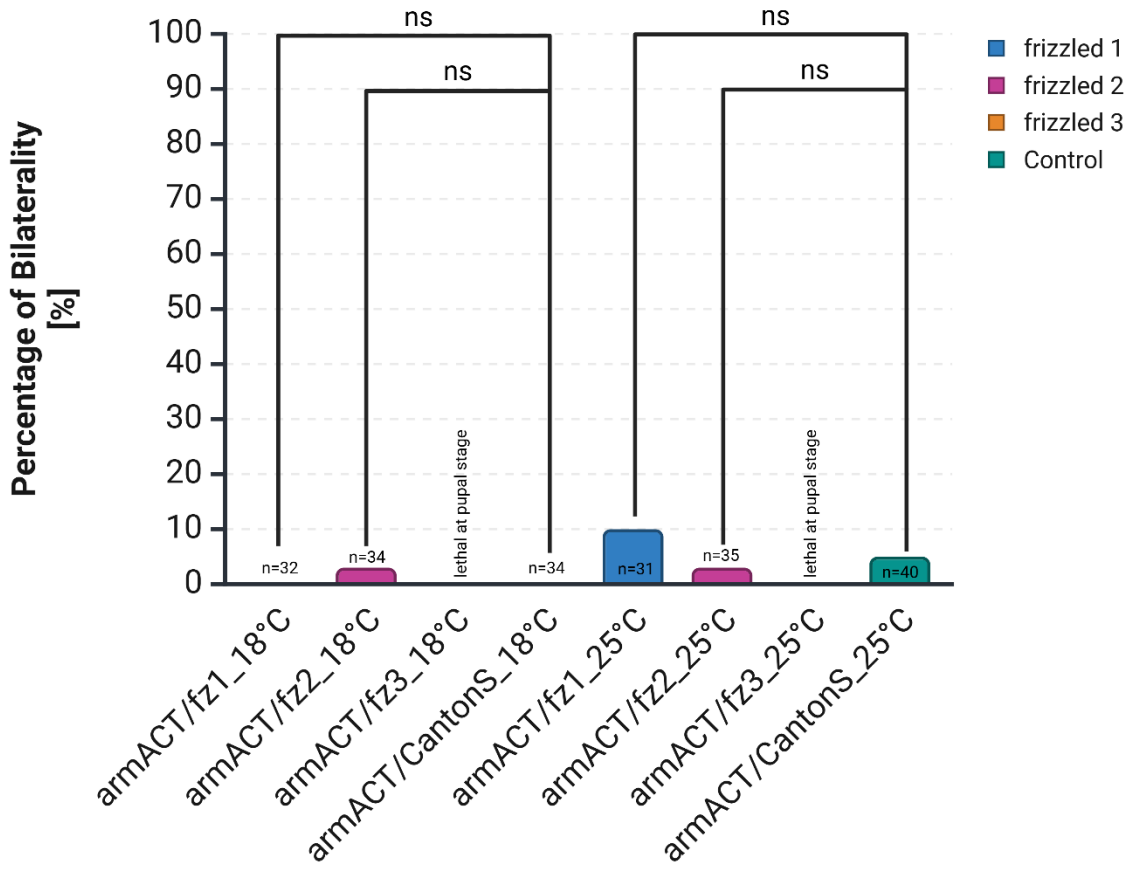

Figure 13: *Armadillo activation in Frizzled expressing cells at 18°C and 25°C. Y-Axis shows the percentage of bilateral phenotypes of SA^{uni}. Control being Canton S crossed with the UAS-arm^{act}. Armadillo activation in Frizzled 3 expressing-neurons causes lethality in flies. No significant effect can be seen. Created in https://BioRender.com*

Activation of Armadillo in the Frizzled 1 ($\frac{+}{UAS-arm^{act}}$;;$\frac{fz-Gal4}{+}$) and Frizzled 2 ($\frac{+}{UAS-arm^{act}}$;;$\frac{fz2-Gal4}{+}$) Gal4 lines also has no significant effect on bilaterality. However, like the FB1B-Gal4 line crossed with UAS-arm^{act}, the Frizzled 3 ($\frac{\mathrm{fz3-Gal}}{\mathrm{UAS-arm^{act}}}$;;$\frac{\mathrm{UAS-y}}{+}$) Gal4 line crossed with it, also results in lethality in the flies, thus its effect on remodelling cannot be determined (Fig.9 and Fig. 13). Overall, the percentages range from 0 to 10 percent, with no significant difference compared to the control ($\frac{+}{UAS-arm^{act}}$;;).

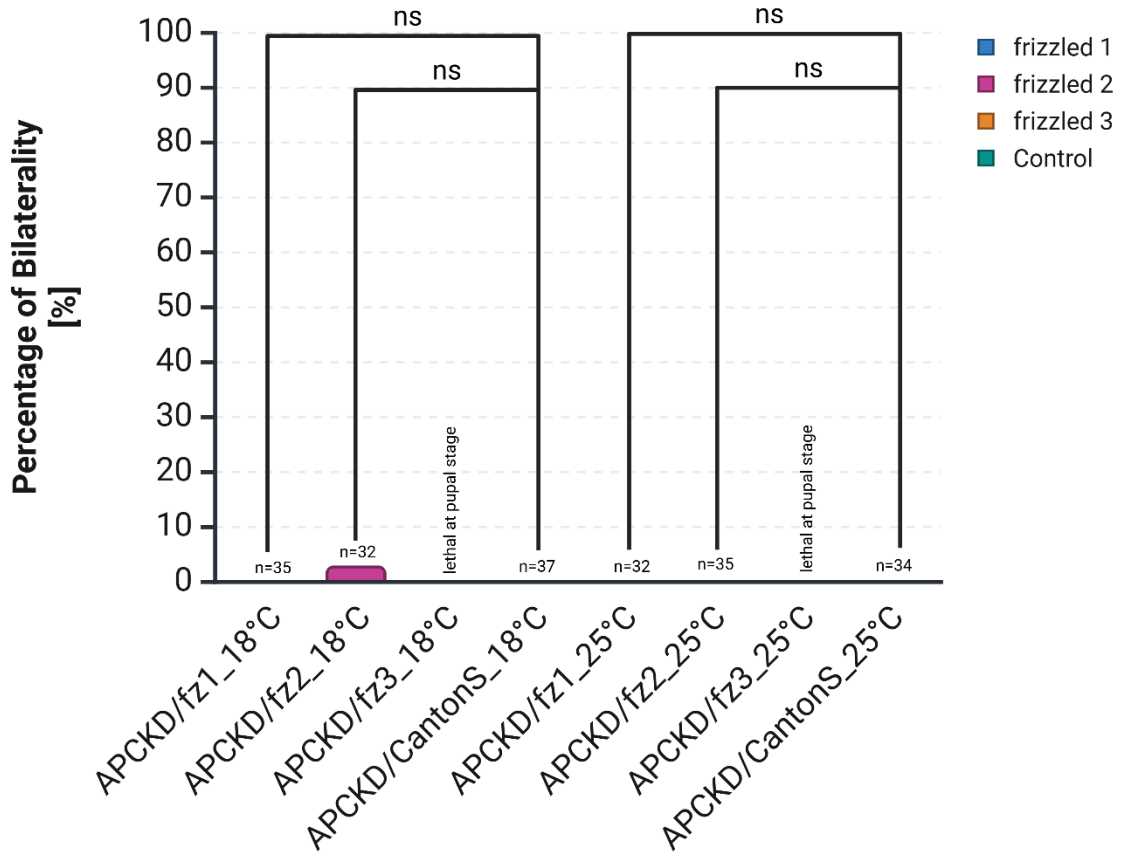

Figure 14: *APC knockdown in Frizzled expressing cells at 18°C and 25°C. Y-Axis shows the percentage of bilateral phenotypes of SAuni. Control being Canton S crossed with the UAS-APC^{RNAi}. APC knockdown in Frizzled 3 expressing-neurons causes lethality in flies. No significant effect can be seen. Created in https://BioRender.com*

When APC is knocked down in Frizzled-expressing cells, the cross for Frizzled 3 ($\frac{fz3-Gal}{+}$; $\frac{+}{UAS-Apc^{RNAi}}$; $\frac{UAS-y}{+}$) leads to early lethality and could not be analysed for the adult AB phenotype (Fig. 14). Aside from this, there are virtually no bilateral phenotypes observed in Frizzled 1 (; $\frac{+}{UAS-Apc^{RNAi}}$; $\frac{fz-Gal4}{+}$), Frizzled 2 (; $\frac{+}{UAS-Apc^{RNAi}}$; $\frac{fz2-Gal4}{+}$) and the Control (; $\frac{+}{UAS-Apc^{RNAi}}$;), indicating that the APC knockdown does not lead to significant developmental abnormalities in the other Frizzled lines.

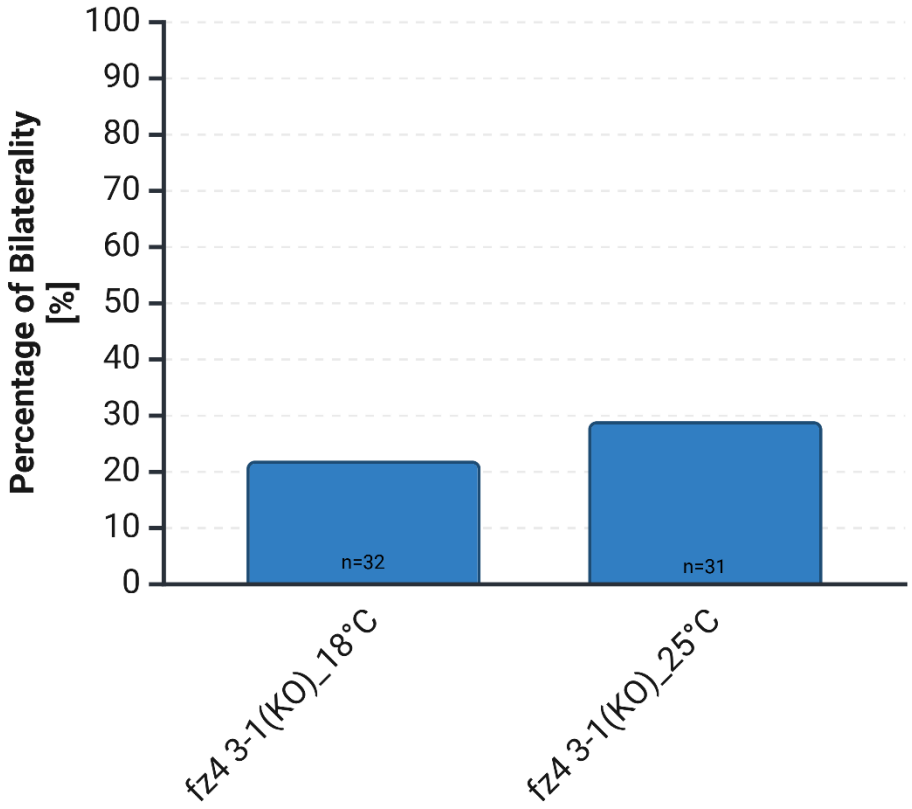

Figure 15: Frizzled 4 Receptor Knockout mutant at 18°C and 25°C. Y-Axis shows the percentage of bilateral phenotypes of SA^{uni}. Created in https://BioRender.com.

Due to time constraint, Frizzled 4 was only investigated through a mutation. The mutation was induced by P-element mobilization by Delta2-3 transposase. Through Imprecise excision of the progenitor insertion a deletion, which removes fz4 sequences, was created, making an amorphic allele (McElwaine et al., 2011).

Additionally, the Frizzled 4 Knockout mutant ($fz4^{3-1}$;;) displays a bilaterality rate of 21% at 18°C, which increases to 29% at 25°C, indicating a slight but consistent temperature-dependent change in its phenotype (Fig. 15).

The data shows that a Knockout of Frizzled 4 could indirectly halt SA^{uni} remodelling.

3.3 Interaction between *wnt4*^{EMS23} and Armadillo

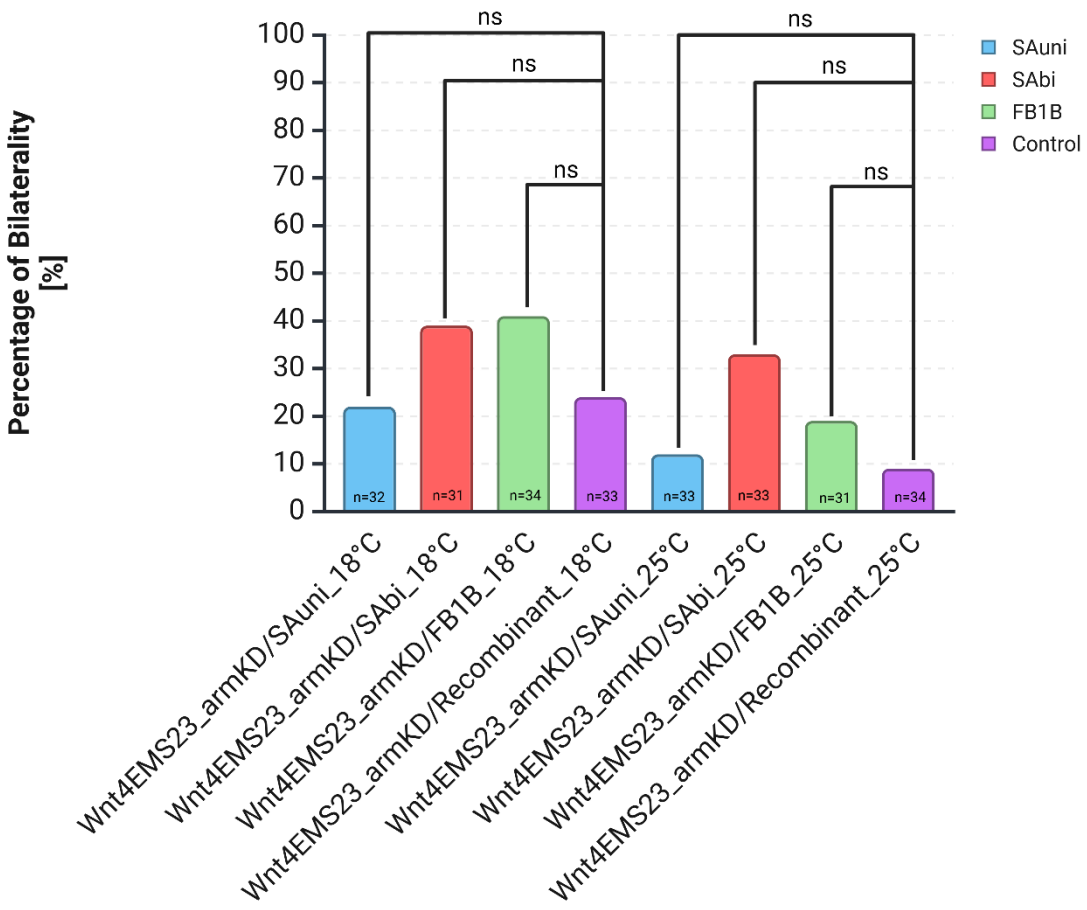

Figure 16: *Armadillo knockdown with wnt4*^{EMS23} *background in AB associated neurons at 18°C and 25°C. Y-Axis shows the percentage of bilateral phenotypes of SA*^{uni}*. Control being SA*^{uni}*-GFP-recombinant crossed with the UAS-arm*^{RNAi} *including the wnt4*^{EMS23} *as a mutant background. No significant effect can be seen. Created in https://BioRender.com*

In isolated *wnt4*^{EMS23} heterozygous flies, the bilateral rate of SA^{uni}-neurons was observed to be approximately 48% when the flies were maintained at 18°C. In contrast, when the temperature was raised to 25°C, the bilateral rate increased to around 75% (Data from Johann Markovitsch and Daniel Mitic). With these isolated lines, a stock was established containing either Armadillo RNAi for knockdown or constant activation of the protein. These stocks were used to investigate the outcome on the AB with the interaction between the mutant and Armadillo.

Armadillo knockdown in wildtype flies resulted in a bilaterality rate ranging from 15 to 25% at 18°C for the AB (Fig. 8). At 25°C, the bilaterality rate was 10% for both control and FB1B neurons, and about 25% for SA^{uni}- and SA^{bi}-neurons. In *wnt4*^{EMS23} heterozygous flies with Armadillo knockdown, the overall rate of bilateral phenotypes increased in

comparison (Fig. 16). Specifically, Knockdown in SA^{uni} Gal4 lines ($;\frac{Wnt4^{EMS^{23}},bw^{1}}{AB1lexA,lexAop::GFP};\frac{\mathrm{R72A10}-Gal4}{UAS-arm^{RNAi}}$) showed the same rate of bilateral phenotypes as the control ($;\frac{Wnt4^{EMS^{23}},bw^{1}}{AB1lexA,lexAop::GFP};\frac{+}{UAS-arm^{RNAi}}$) at both temperatures. At 18°C, SA^{bi} Gal4 lines ($;\frac{Wnt4^{EMS^{23}},bw^{1}}{AB1lexA,lexAop::GFP};\frac{\mathrm{R66A02}-Gal4}{UAS-arm^{RNAi}}$) and FB1B Gal 4 lines ($;\frac{Wnt4^{EMS^{23}},bw^{1}}{AB1lexA,lexAop::GFP};\frac{\mathrm{R16}E08-Gal4}{UAS-arm^{RNAi}}$) showed a 15% increase in bilaterality compared to controls. At 25°C, SA^{bi} showed a 25% increase in bilaterality over the control, and statistical analysis ($X^2 = 4.6937$, df = 1, p-value = 0.030, N = 67) indicated a significant difference. However, after correcting for multiple tests (Bonferroni correction: p-adjusted = 0.09), the difference was no longer significant.

When compared to wildtype flies (Fig. 8), only the experimental group showed a difference. The bilaterality rate for all experimental groups at 18°C increased by 10-20%, suggesting a tendency for higher bilaterality in the mutant background. At 25°C, SA^{uni}-neurons showed a 15% decrease in bilaterality, while the other experimental groups exhibited a 10% increase.

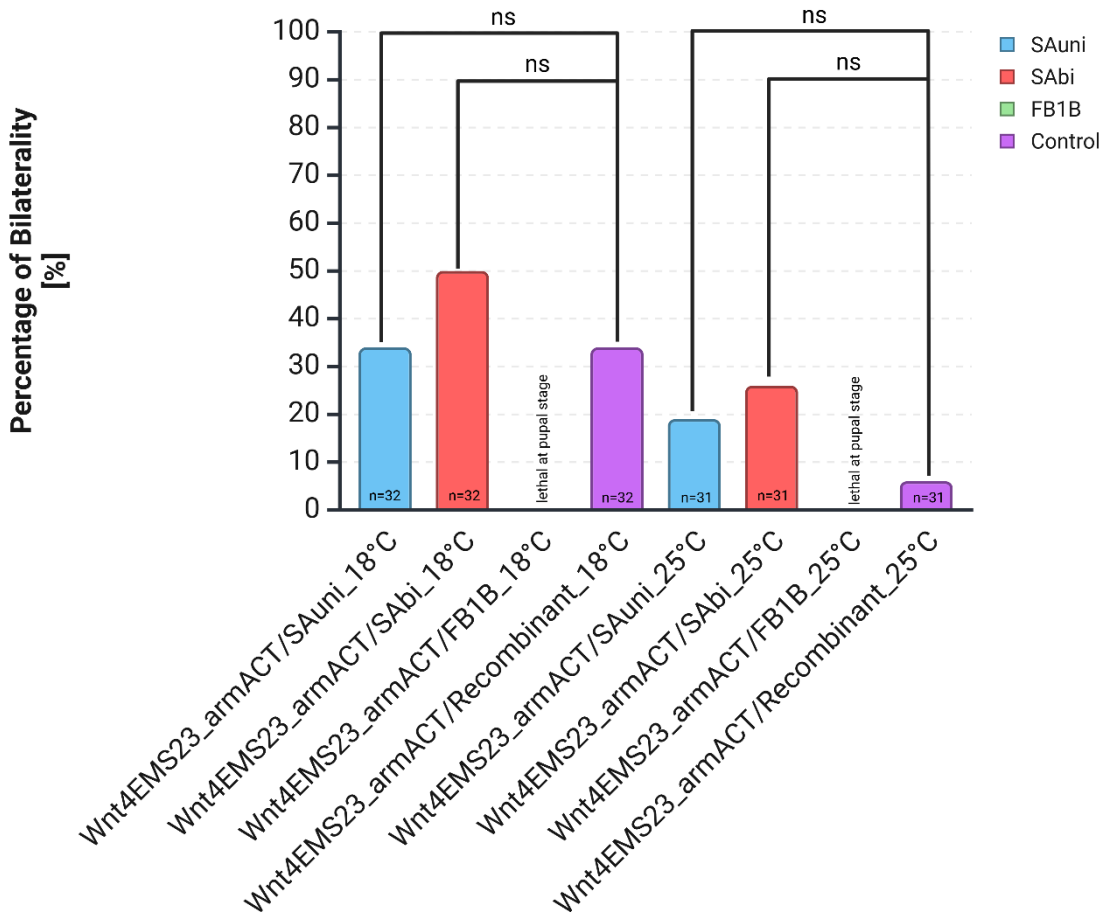

Figure 17: *Armadillo activation with wnt4^{EMS23} background in AB associated neurons at 18°C and 25°C. Y-Axis shows the percentage of bilateral phenotypes of SA^{uni}. Control being SA^{uni}-GFP-recombinant crossed with the UAS-arm^{act} including the wnt4^{EMS23} as a mutant background. Armadillo activation in FB1B-neurons causes lethality in flies. No significant effect can be seen. Created in https://BioRender.com*

Armadillo activation in wildtype flies proved lethal for FB1B neurons. At 18°C, the bilaterality rate for SA^{uni}-neurons was 15%, while the control and SA^{bi}-neurons showed a bilaterality rate of around 30%. At 25°C, all three groups exhibited a bilaterality rate within the range of 20-25%.

Similar to the normal Armadillo activation in the AB-associated Gal4 lines, activating Armadillo in this case is also lethal for the FB1B line ($\frac{UAS-arm^{act}}{+}$; $\frac{Wnt4^{EMS^{23}},bw^{1}}{AB1lexA,lexAop::GFP}$; $\frac{R16E08-Gal4}{+}$) (Fig. 17). Otherwise, both the Control ($\frac{UAS-arm^{act}}{+}$; $\frac{Wnt4^{EMS^{23}},bw^{1}}{AB1lexA,lexAop::GFP}$;) and SA^{uni} ($\frac{UAS-arm^{act}}{+}$; $\frac{Wnt4^{EMS^{23}},bw^{1}}{AB1lexA,lexAop::GFP}$; $\frac{R72A10-Gal4}{+}$) crosses show a bilaterality rate of 33% at 18°C, with SA^{bi} ($\frac{UAS-arm^{act}}{+}$; $\frac{Wnt4^{EMS^{23}},bw^{1}}{AB1lexA,lexAop::GFP}$; $\frac{R66A02-Gal4}{+}$) exhibiting a slightly higher rate of 50%. At

25°C, the bilaterality rate decreases across all lines: SAuni at 18%, SA^{bi} at 25%, and the Control at 6%.

When comparing the flies with *wnt4*^{EMS23} to the ones without this mutation (Fig. 9), the experimental groups SA^{uni} and SA^{bi} show an approximate 20% increase in bilateral phenotypes in flies with the *wnt4*^{EMS23} mutated background at 18°C. However, at 25°C, the control group exhibits a decrease of about 15% in bilateral phenotypes, indicating a temperature-dependent variation in the expression of bilaterality between the mutated and control groups.

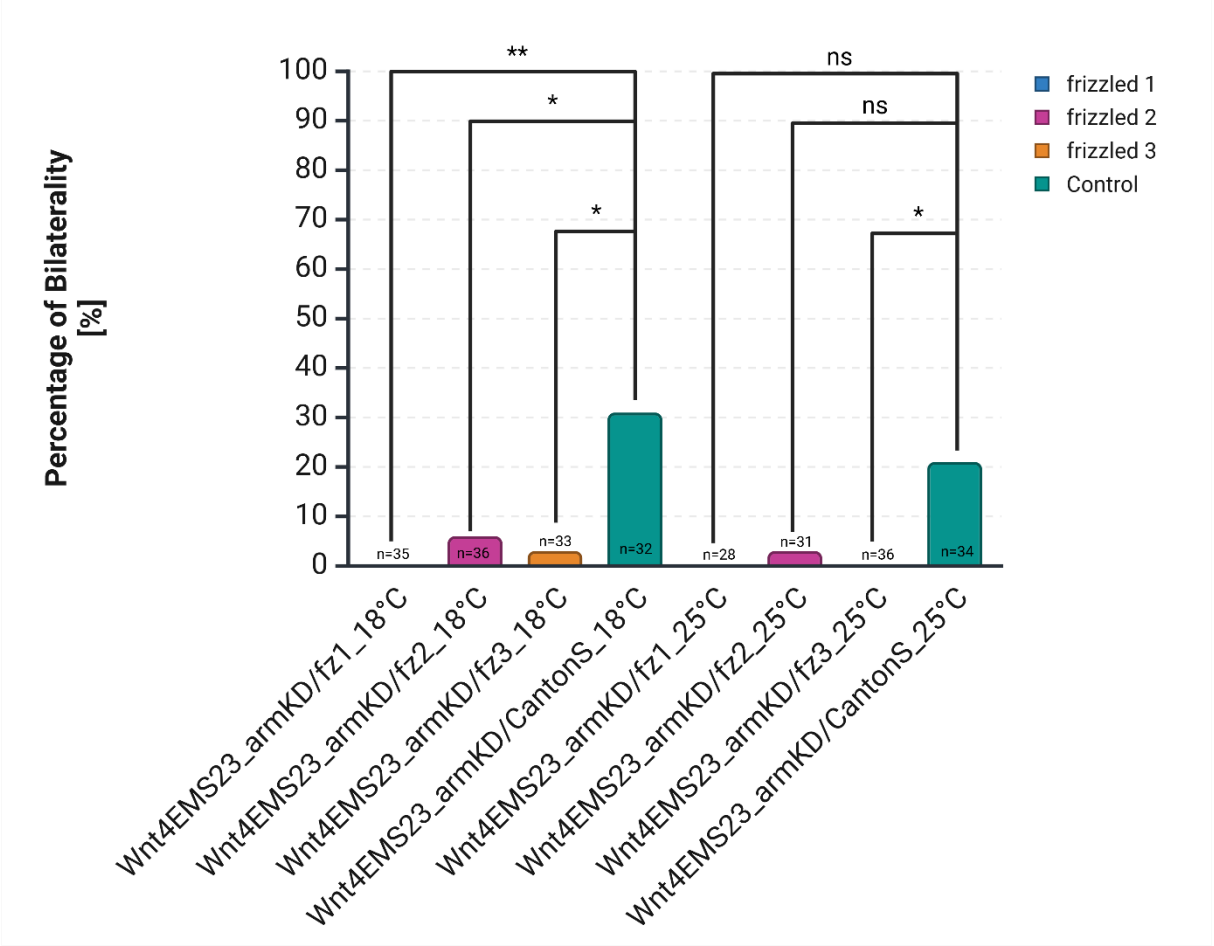

Figure 18: *Armadillo knockdown with wnt4*^{EMS23} *background in Frizzled expressing neurons at 18°C and 25°C. Y-Axis shows the percentage of bilateral phenotypes of* SA^{uni}*. Control being Canton S crossed with the UAS-arm*^{RNAi} *including the wnt4*^{EMS23} *as a mutant background. At 18°C all experiments were significantly different to the control. However, at 25°C only Fz3 shows a significant difference. Created in https://BioRender.com*

Armadillo knockdown in Frizzled-expressing cells resulted in a bilaterality rate ranging from 0% to 10% (Fig. 12).

All three Frizzled Gal4 lines show a notable difference when Armadillo is knocked down in a heterozygous *wnt4^{EMS23}* mutant background at 18°C (Fig. 18). Frizzled 1 (; $\frac{Wnt4^{EMS^{23}},bw^{1}}{+}$; $\frac{\mathrm{fz}-Gal4}{UAS-arm^{RNAi}}$) shows a 30% difference compared to the control, with a highly significant result (X-squared = 10.513, df = 1, p-value = 0.001, n = 67). Frizzled 2 (; $\frac{Wnt4^{EMS^{23}},bw^{1}}{+}$; $\frac{\mathrm{fz2}-Gal4}{UAS-arm^{RNAi}}$) shows a modest but significant decrease compared to the control (X-squared = 6.0296, df = 1, p-value = 0.014, n = 68). Frizzled 3 ($\frac{fz3-Gal}{+}$; $\frac{Wnt4^{EMS^{23}},bw^{1}}{+}$; $\frac{\mathrm{UAS-y}}{UAS-arm^{RNAi}}$) also exhibits a slight, significant reduction relative to its control (X-squared = 7.3045, df = 1, p-value = 0.007, n = 65). At 25°C, only Frizzled 3 (X-squared = 6.1066, df = 1, p-value = 0.013, n = 70) demonstrates a slight but significant difference from the control. Due to the Bonferroni correction Frizzled 1 only shows a tendency at 25°C.

When comparing the bilateral phenotypes of Armadillo knockdown in Frizzled-expressing cells (Fig. 12) to these data, in general the control groups show a higher bilaterality rate by approximately 20% higher at both experimental temperatures.

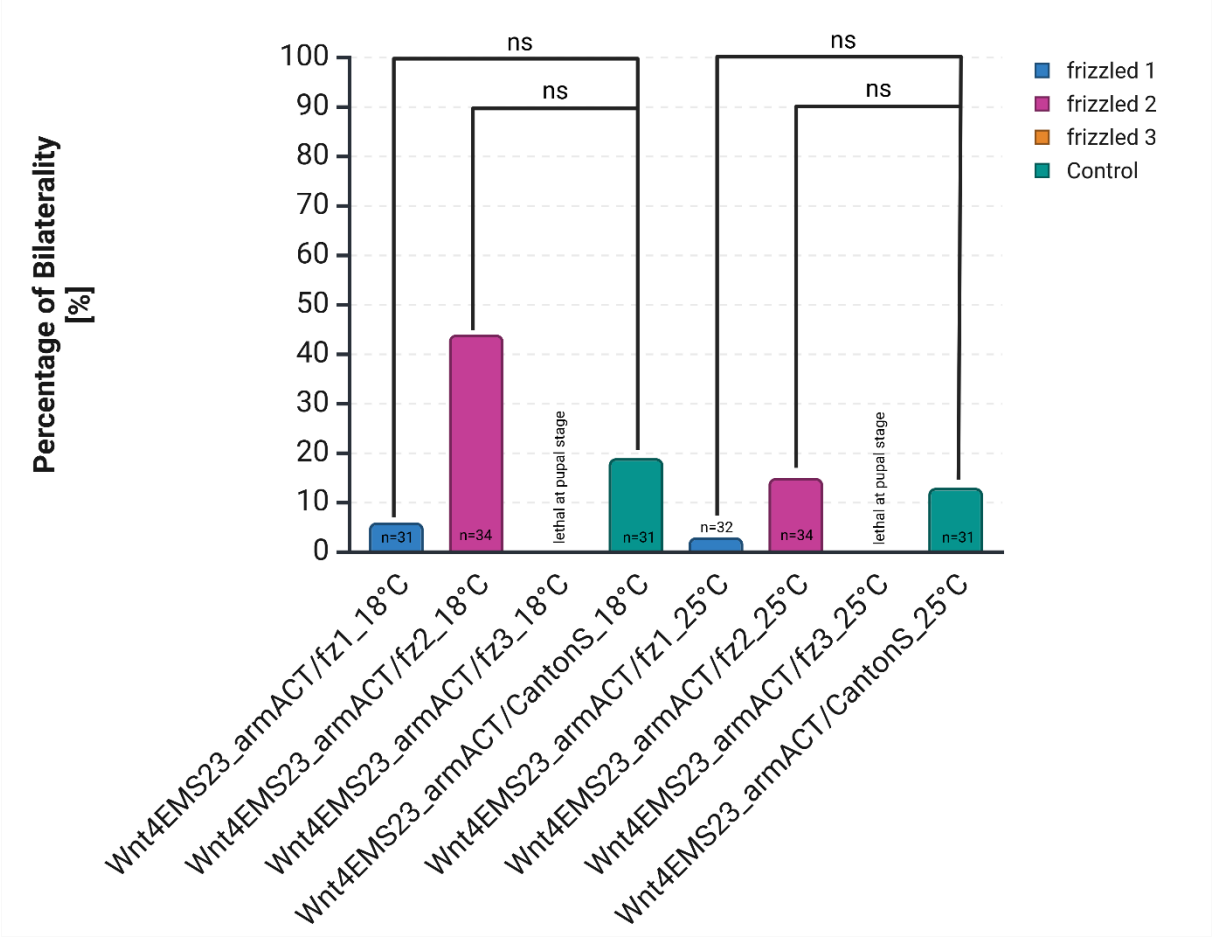

Figure 19: *Armadillo activation with wnt4^{EMS23} background in Frizzled expressing neurons at 18°C and 25°C. Y-Axis shows the percentage of bilateral phenotypes of SA^{uni}. Control being Canton S crossed with the UAS-arm^{act} including the wnt4^{EMS23} as a mutant background. Armadillo activation in Fz3 expressing neurons causes lethality in flies. No significant effect can be seen. Created in Created in https://BioRender.com*

Armadillo activation in Frizzled-expressing cells also resulted in a bilaterality range from 0% to 10% at both experimental temperatures (Fig.13). However, the cross involving Fz3 turned out to be lethal.

When Armadillo is activated in Frizzled-expressing cells within a *wnt4^{EMS23}* heterozygous background, no significant difference is observed compared to the control (Fig. 19). It is worth noting that, although none of the lines show a statistically significant difference, Frizzled 2 ($\frac{+}{UAS-arm^{act}}$; $\frac{Wnt4^{EMS^{23}},bw^{1}}{+}$; $\frac{fz2-Gal4}{+}$) tends to be approximately 25% higher than its control ($\frac{UAS-arm^{act}}{+}$; $\frac{Wnt4^{EMS^{23}},bw^{1}}{+}$;) at 18°C. Similar to the activation with normal background, Frizzled 3 ($\frac{fz3-Gal}{UAS-arm^{act}}$; $\frac{Wnt4^{EMS^{23}},bw^{1}}{+}$; $\frac{UAS-y}{+}$) is lethal with the mutant

background as well. Frizzled 1 ($\frac{+}{UAS-arm^{act}}$; $\frac{Wnt4^{EMS^{23}},bw^{1}}{+}$; $\frac{fz-Gal4}{+}$) shows a reduction of bilateral phenotypes at both temperature of about 10 percent compared to the control.

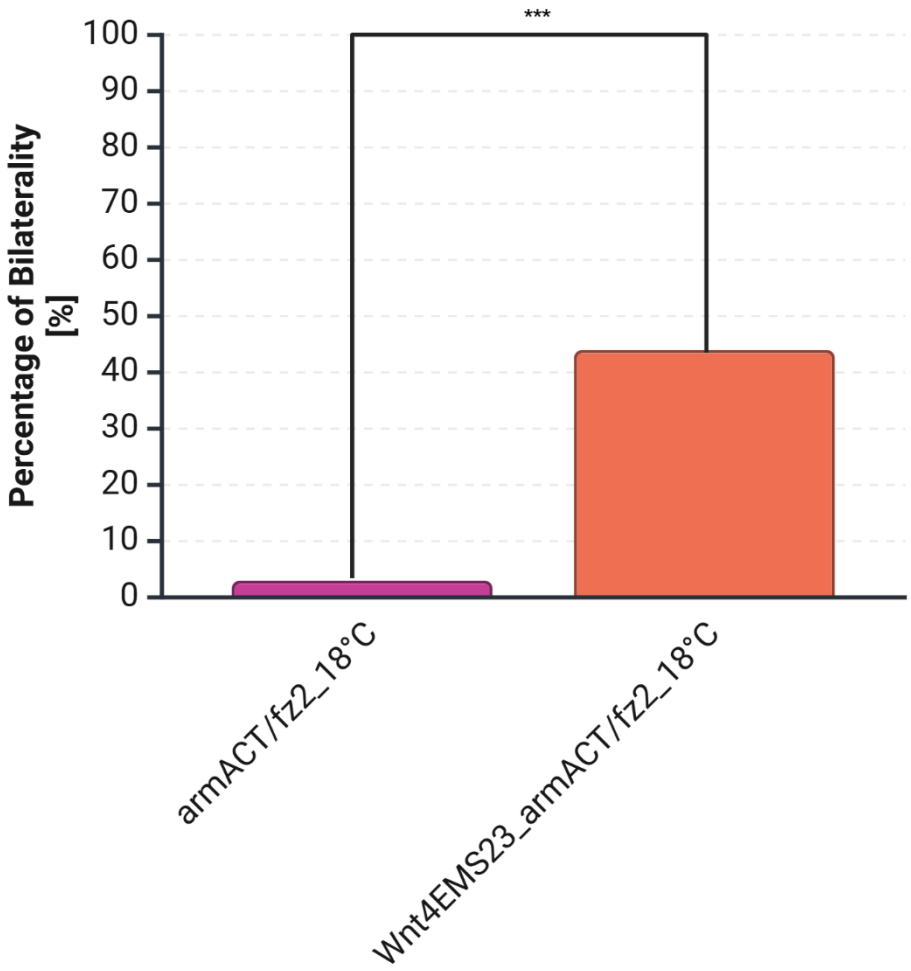

Figure 20: *Comparison of frizzled 2 enhancer driven armadillo activation with Wnt4EMS2-background. Y-Axis shows the percentage of bilateral phenotypes of SA^{uni}. Statistical comparison two experimental groups ($\frac{+}{UAS-arm^{act}}$; ; $\frac{fz2-Gal4}{+}$) and ($\frac{+}{UAS-arm^{act}}$; $\frac{Wnt4^{EMS^{23}},bw^{1}}{+}$; $\frac{fz2-Gal4}{+}$). Created in https://BioRender.com.*

When comparing the percentage of bilateral AB phenotypes through armadillo activation (Fig. 13) in Frizzled 2 to the same activation with Wnt4^{EMS23}, notably, expression in Fz2-Gal4 demonstrates a highly significant difference (X-squared = 12.838, df = 1, p-value = 0.0003397, n = 67) (Fig. 20). In neurons expressing Frizzled 2, armadillo activation causes a 40% higher bilaterality AB rate when the Wnt4^{EMS23} mutant background is present, compared to when it is absent. In comparison the control of armadillo activation with CantonS shows a slighter difference to armadillo activation with CantonS in Wnt4^{EMS23} mutants. With the mutant background the bilaterality rate of the AB is approximately 20% higher at 18°C.

3.4 Co-receptor Knockout effects on the AB

Wnt molecules often do not bind solely to Frizzled receptors; co-receptors are as mentioned also often needed. In this chapter, various knockout mutants are tested to determine whether they are involved in the remodelling of the AB. *Arrow*^{2} is a mutant which was induced by exposure of ethyl methane sulfonate (Tearle and Nusslein-Volhard, 1987). Through this a premature stop codon is introduced between EGF-like repeats 2 and 3, making a Knockout mutant (Wehrli et al., 2000). *Nrk*^{KO} is a mutant created through CRISPR/Cas9. Most of its endogenous coding sequence was deleted, making it a loss of function allele (Fradkin, 2023). Lastly *Ror*^{4} is a mutation induced by P-element activity. Through the deletion most of the sequence including the start codon and most of the first three exons of Ror were removed (Ripp et al., 2018).

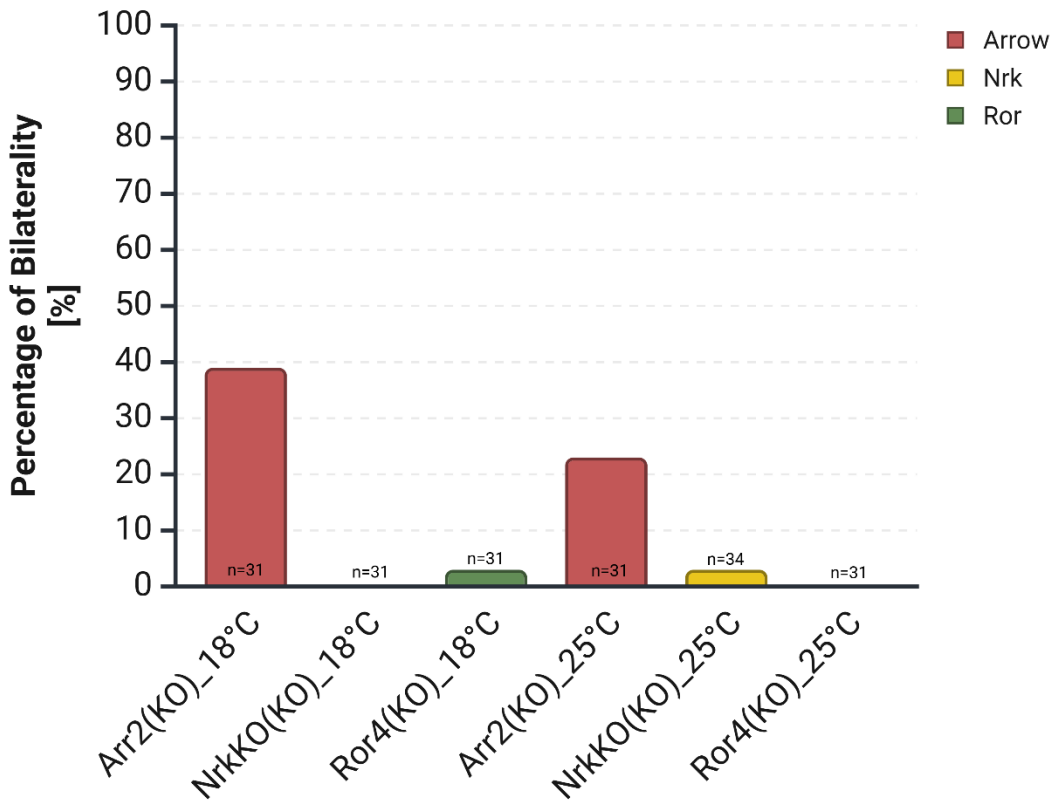

Figure 21: *Percentage of SAuni bilaterality in Co-receptor Mutants at 18°C and 25°C. Arr (Arrow), Nrk (Neurospecific receptor kinase) and Ror (RTK-like orphan receptor) are Co-receptors. The Y-Axis shows the percentage of bilateral phenotypes of SAuni. Arrow and Fz4 shows a heightened bilaterality rate. Created in https://BioRender.com*

Among the co-receptors tested, only heterozygous *arrow*^{2} *mutants* (; $\frac{ch^1,arr^2,bw^1,speck^1}{Cyo}$;) exhibits an increased bilateral AB rate (Fig. 21). When comparing arrow to the other co-receptors, Ror (; Ror^4;) and Nrk (; Nrk^{KO};), a noticeable difference of 35–40% higher bilaterality rate is observed at 18°C. At 25°C the difference decreases to 20% for the bilateral phenotypes.

The fact that the Arrow mutant is heterozygous yet still exhibits a strong effect suggests a dominant phenotype.

This data implies that Arrow has an effect on the remodelling of SA^{uni}-neurons. However, in this case a knockout of said co-receptor causes the halt on remodelling, raising the question if it works in an antagonistic fashion to Fz2 or having a role outside of the Canonical Wnt Signalling Pathway.

4. Discussion

Do the findings show that *wnt4*^{EMS23} a gain-of-function mutant as hypothesized?

Firstly, the expression of Wnt4 and the frizzled receptors do not overlap with the AB, but Wnt4 and Frizzled 3 show an overlap of expression in the fan shaped body. A key finding of this study is that Armadillo activated in Frizzled 2 expressing glial cells increases bilaterality rate of the AB only in the presence of the *wnt4*^{EMS23} mutant background. This showed that Wnt4 has no function for this specific remodelling in wildtype flies. Another a significant and independent discovery is that knocking down APC in SA^{bi} neurons results in a high rate of bilaterality in SA^{uni} neurons. Lastly a Co-receptor Knockout mutant of arrow (*arr*^{2}) and a receptor Knockout of Frizzled 4 (*fz4*$^{3-1}$) showed an increased bilateral AB rate.

These data showed that the activation of Armadillo in Frizzled 2 expressing neurons, in combination with the *wnt4*^{EMS23} mutant, increases the percentage of bilaterality immensely.

Isolated *wnt4*^{EMS23} mutants with UAS-arm^{act} crossed with CantonS showed a bilateral AB Fas2 expression of about 15%. Following the interference of Armadillo function in Frizzled 2 expression cells it increased to about 45%. Indicating the importance of the interaction between Wnt4, Frizzled 2 and Armadillo.

Interestingly, when armadillo is activated in the fz2 expressing neurons, it does not lead to the cessation of the remodelling process on its own. This suggests that while armadillo activation is a crucial component of the signalling cascade, its activation in this context is not sufficiently robust or potent to directly halt the remodelling process. It indicates that additional factors or signals may be necessary to amplify the armadillo response, or that the activation of armadillo in this specific context may not fully mimic the physiological conditions required to halt remodelling.

This data suggests that the *wnt4*^{EMS23} mutant is a gain-of-function mutant as hypothesised, due to the increase of bilateral SA^{uni} phenotypes in armadillo activated frizzled 2 expressing cells, when *wnt4*^{EMS23} is present. Thus, Canonical Wnt Signalling plays a key role in regulating the asymmetric remodelling of SA^{uni} neurons.

A reduction in APC within SA^{bi} neurons may interfere with normal asymmetric development, leading to a more symmetric phenotype in SAuni neurons. This process appears not to involve Wnt Signalling but may instead be mediated through the cytoskeleton. This is a non-autonomous effect. SA^{bi} is known to be a progenitor neuron for SA^{uni}. This means the interference in SA^{bi} neurons can inevitably cause the interference in SAuni neurons as well.

Arrow most likely plays a role in the remodelling outside of the Canonical Wnt Signalling Pathway. Due to the fact, that its Knockout causes the heightened effect of bilateral phenotypes in the AB.

4.1 Armadillo activated in specific Glia affect the Remodelling of SAuni neurons

Glia plays a crucial role in guiding neuronal remodelling. Research has demonstrated that glia secretes Myoglianin, a TGF-β ligand, which directs neural remodelling in the mushroom bodies (ref). It has been shown that glia coordinate developmental neural remodelling not only through the engulfment of excess neurites but also by facilitating neuronal remodelling. By knocking down Myoglianin in larval cortex and astrocyte-like glial cells, thus causing a disruption of the TGF-ß signalling, the remodelling process of mushroom bodies was halted during pupal stage (Awasaki et al., 2011). The same glia celltypes are known to be present in the central complex, making it possible to have an influence on the remodelling of the SA^{uni}-neurons (Marc Freeman, 2015).

Wnt4 could be secreted and collected by glia through Frizzled 2 receptors. This causes a down cascade resulting in gene expression which causes the secretion of Myoglianin from the cells.

Myoglianin, when bound to the Babo receptor, is known to trigger the phosphorylation of Mad (Mothers against dpp), among other effects. Mad is an R-Smad (receptor-activated Smad) that transmits the BMP (Bone Morphogenetic Protein) Signalling Pathway. Mad is also known to form a complex with Armadillo, which regulates the expression of Wnt target genes (Upadhyay et al., 2017).

When Armadillo is activated in glia expressing Frizzled 2 receptors, it leads to a disruption in the remodelling of the AB. This effect occurs only when excess Armadillo is present in conjunction with the $Wnt4^{EMS23}$ background. This observation suggests that

Armadillo and Mad might collaborate in regulating the target genes that drive the remodelling process. Their combined activity may play a crucial role in coordinating the molecular signals necessary for proper neuronal remodelling. By cooperating, Armadillo and Mad could influence the expression of specific genes that are involved in the structural changes required for neural development and adaptation.

4.2 APC involvement in Remodelling of SA^{uni} neurons

APC knockdown in SA^{bi} neurons disrupts the remodelling of the SA^{uni} neurons. The lack of disruption caused by active Armadillo in SA^{bi} neurons suggests APC has a function independent of the canonical Wnt signalling pathway.

Canonical Wnt Signalling is not its only role, as a wide range of other partners have been identified over the years (Abbott and Näthke, 2023). Over a hundred interaction partners have been revealed, its involvement being in diverse cellular processes including Migration, Adhesion, Transpost, Gene expression, Protein synthesis, Cell division and Life and death (Nelson and Näthke, 2013).

Although APC is most prominently known for the Wnt Signalling Pathway, it is also a regulator for the cytoskeleton with links to both actin and myosin (Fang and Svitkina, 2022).

A possible function of SA^{uni} remodelling is through the signal from SA^{bi} which does cell migration through the cytoskeleton. Actin filaments, often with myosin, drive many cell movements. Myosin, a molecular motor, converts ATP into mechanical energy, generating force and movement. While muscle contraction is the most notable example, actin-myosin interactions also drive various nonmuscle cell movements, including cell division, playing a key role in cell biology. Additionally, the actin cytoskeleton enables cell crawling, powered by actin polymerization and actin-myosin interactions, which is significant for neurons (Cooper, 2000).

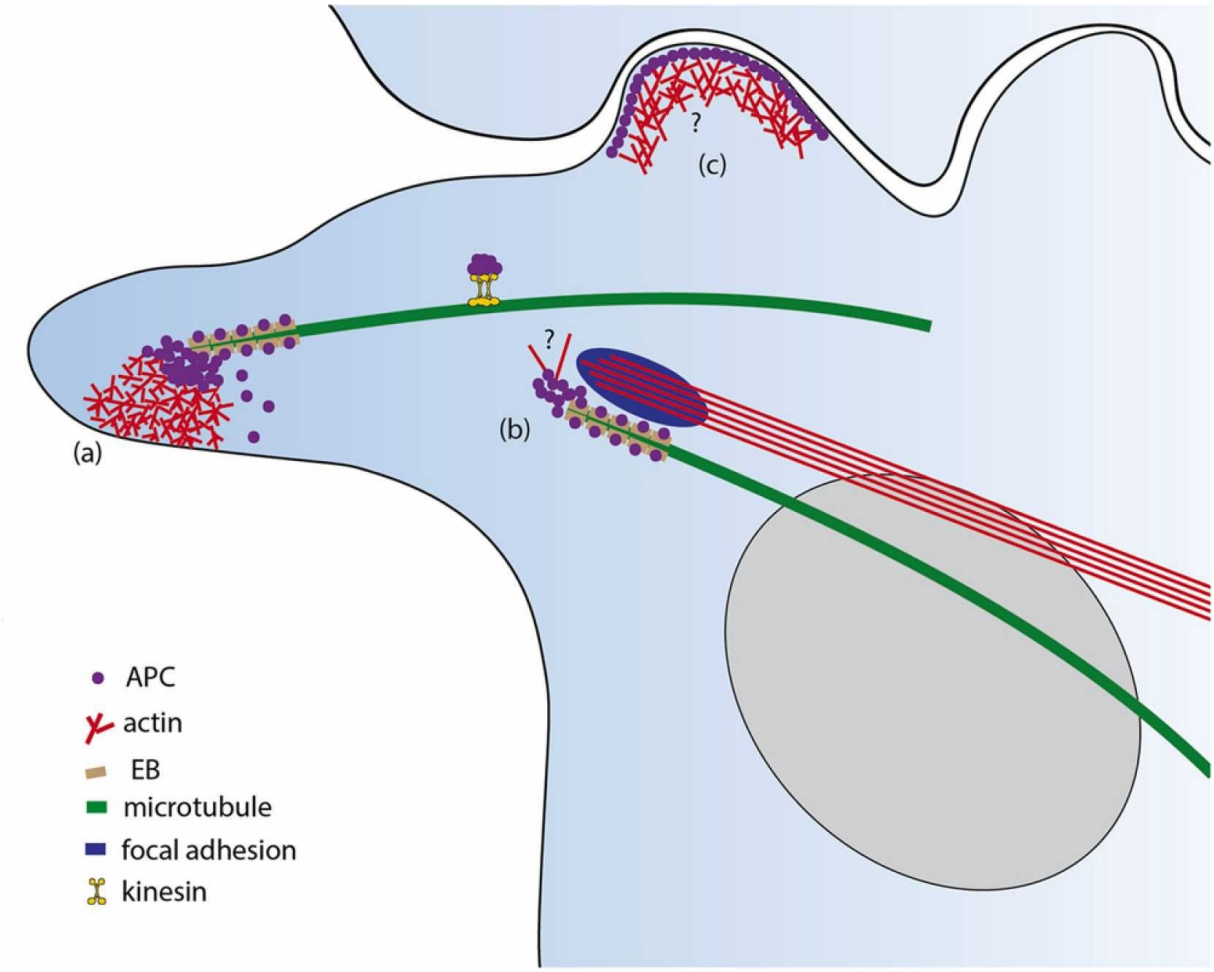

Figure 22: *APCs functions and localisation in cell migration. (a) APC clusters at microtubule tips trigger branched actin assembly at the cell's leading edge for membrane protrusion. (b) APC clusters near focal adhesions nucleate linear actin filaments, promoting focal adhesion turnover via an unknown mechanism. (c) APC can localize to cell-cell junctions, but its role there is unclear. APC accumulates at microtubule tips through interactions with EB family +TIPs or kinesin motors. (Made by Fang and Svitkina, 2022).*

APC regulates both actin and microtubules (Fig. 22) stabilizing microtubules while maintaining their dynamics at the plus ends. It also promotes actin-based protrusion by activating the APC-Cdc42-N-WASP-Arp2/3 complex pathway. Additionally, APC appears to enhance focal adhesion dynamics, though the mechanism remains unclear (Fang and Svitkina, 2022).

APC stabilizes microtubules by binding to their lattice via its basic domain, with support from the APC-EB1 interaction. In terms of actin, APC seems to have several roles. It is thought to facilitate communication between microtubules and contractile actin bundles linked to focal adhesions. Given that membrane protrusion at the leading edge is driven by actin polymerization through the Arp2/3 complex, this suggests APC also helps coordinate microtubules with protrusive branched actin networks. Such

coordination is crucial for accurate cell migration, particularly in neurons, which grow neurites over long distances to precise targets, forming functional neural circuits during development and after injury. The high levels of APC expression in the brain, along with the neuron-specific APC2 paralog, emphasize APC's central role in cell polarity and navigation (Fang and Svitkina, 2022).

To conclude the data possibly points APC to have a cell migratory role in the remodelling of SAuni neurons, either by collaborating with actin or myosin, through the migration of SAbi.

4.3 Arrow's possible functions in remodelling of neurons

The absence of LRP5/6 leads to various defects in humans, including an association with Alzheimer's disease and abnormalities in the central nervous system (Joiner et al., 2013). LDL receptor-related proteins 5 and 6 (LRP5/6), along with their Drosophila homolog Arrow, are essential single-span transmembrane proteins that act as co-receptors in the Canonical Wnt Signalling Pathway (Tamai et al., 2004).

In LRP6 mutant mice, reduced production of dentate granule neurons and abnormalities in radial glial scaffolding were observed (Zhou et al., 2004). Glia are known to play a role in neuronal remodelling, and mutations disrupting the scaffolding could impair this process, leading to increased bilateral phenotypes of SA^{uni}.

Arrow's role as a co-receptor was thought to be its sole function, but recent findings suggest it may also have an additional role (Han et al., 2020), potentially explaining the decreased remodelling when Arrow is absent. Exosomal Arrow appears to elevate the extracellular levels of Sol narae (Sona) independently of Wnt Signalling. In arr2 $(; \frac{ch^1,arr^2,bw^1,speck^1}{Cyo};)$ mutants, extracellular Sona levels were found to be reduced. A proposed model suggests that Arrow, secreted via extracellular vesicles (EVs), signals early endosomes to regulate Sona secretion through EVs or direct it toward lysosomal degradation (Han et al., 2020).

Sona, a member of the ADAMTS (A Disintegrin And Metalloprotease with ThromboSpondin motif) family, is thought to enhance Wnt Signalling by promoting its

secretion. Its primary function is to generate the Wg(-CTD) C-terminal domain, which is believed to stabilize cytoplasmic Armadillo and interact with other components of the Canonical Wnt Signalling Pathway (Won et al., 2019). However, further research is needed to determine whether Sona has additional functions outside of Wg.

These findings suggest that Arrow is necessary in certain neurons to activate the Canonical Wnt Signalling Pathway, initiating the remodelling process. This could have a non-autonomous effect on SA^{uni} remodelling, as we know that direct manipulation of the Canoninal Wnt Signalling Pathway has no effect on it.

4.4 hypothesized model

By combining all the gathered data, a model (Fig.23) was created to explain the observed processes and interactions between the cells.

In wildtype the presence of Wnt4 is insufficient to cause significant binding to the Fz2 receptors located on glial cells. As a result, the downstream signalling cascade is not activated, and the Dishevelled protein does not inhibit the Axin complex. Consequently, the Axin complex remains active and continues to phosphorylate Armadillo, leading to its degradation. Because of this ongoing degradation, Armadillo cannot accumulate and translocate to the nucleus, where it would normally interact with transcription co-factors (TCF) to initiate specific gene expression. Without this the remodelling process of SA^{uni}-neurons proceeds normally and the neurons continue their typical development without the alterations seen in conditions where an increased amount of Wnt4 is released.

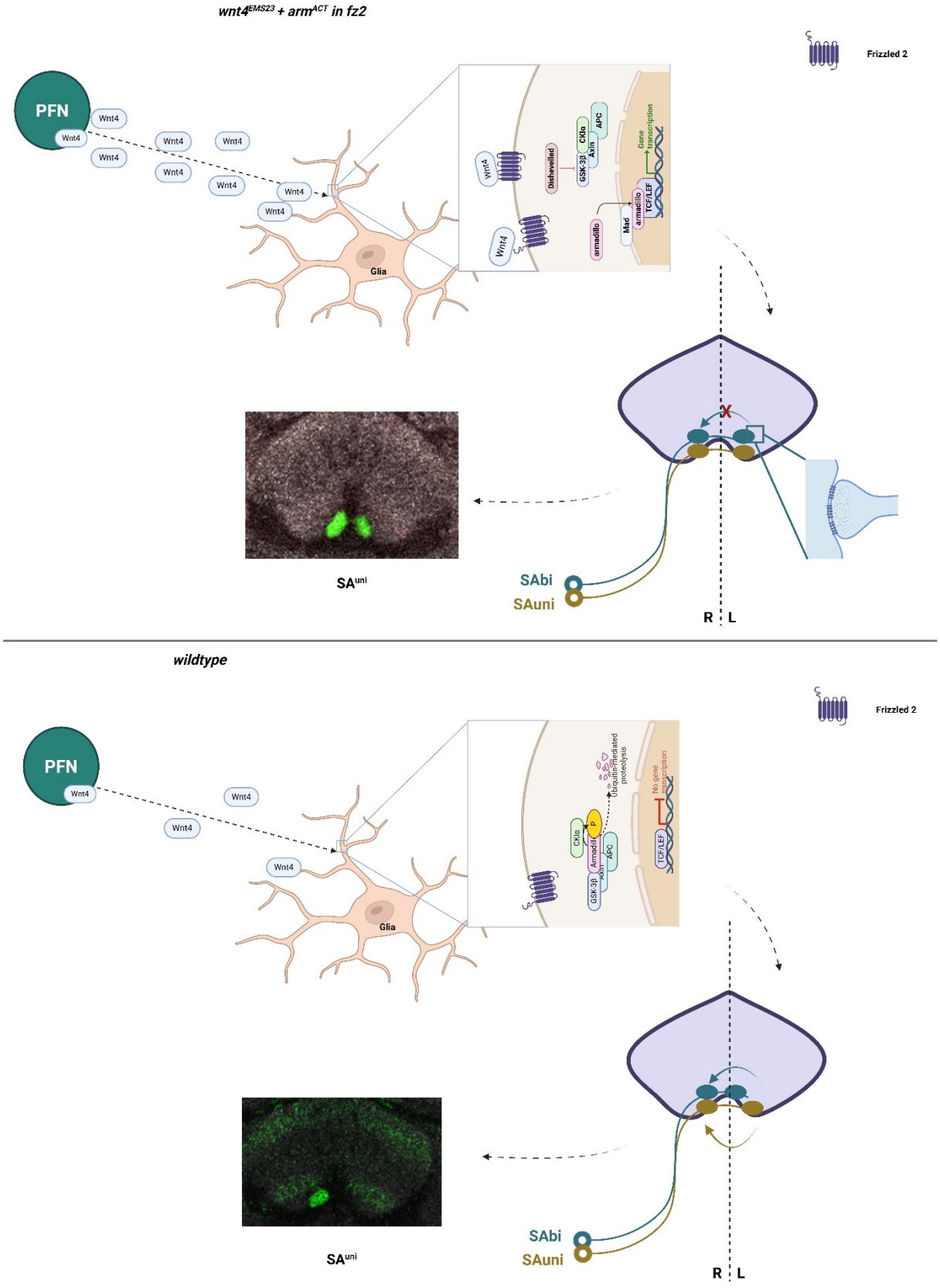

Figure 23: *Model of Remodelling SA^{uni}-neurons in the presence of wnt4^{EMS23} mutation and wildtype background. An active Canonical Wnt Signalling Pathway in wnt4^{EMS23} flies halts the remodelling process of SA^{uni}-neurons. Created in https://BioRender.com*

In *wnt4*^{EMS23} mutants, Wnt4 is secreted from PFNs (protocerebral bridge Fan shaped body neurons) and to Fz2 receptors, which are positioned on glia cells. This interaction activates Dishevelled, which in turn inhibits the Axin complex, preventing it from phosphorylating and degrading Armadillo (the Drosophila homolog of β-catenin). As a result, Armadillo is stabilized, translocates to the nucleus, and binds with Mad to transcription co-factors like TCF (T-cell factor), triggering the activation of specific target genes. This causes the glia to send a signal, anchoring SA^{bi} prematurely in the tissue through synapse formation. This prevents a signal being send to SA^{uni} to retreat itself to the right side, thus staying bilateral.

Glia cells are known for synaptic formation. Them being activated could cause an early anchoring of SA^{bi} neurons in the tissue which are hypothesised to initiate the remodelling in SA^{uni} neurons through synapses. This could prevent it from retreating later in development.

4.5 Next Steps

There are still numerous unresolved questions in this research and addressing them will require additional investigation and experimentation. To clarify some of these uncertainties, I propose several further experimental approaches.

First, the crosses that previously resulted in lethal outcomes should be repeated, this time using the Gal80 system. The advantage of this system is that it allows for precise temporal control over gene activation and knockdown at specific time points. By implementing the Gal80 system, activation or knockdown can be targeted shortly before the remodelling process begins, potentially saving the offspring from death by more accurate timing of gene expression.

Additionally, to more conclusively exclude the involvement of APC in the Canonical Wnt Signalling Pathway in SA^{bi} neurons, it would be beneficial to pair the APC knockdown with an Armadillo knockdown. Armadillo is a crucial component of the Wnt pathway, and by knocking it down alongside APC, we could investigate whether this results in an antagonistic effect on the remodelling process. Conversely, if remodelling does not occur as expected, it would suggest that APC's role in this pathway is more critical than

initially thought. This experiment could provide a clearer understanding of APC's specific function in these neurons.

The results so far indicate that APC is involved in far more processes than originally explored, suggesting that its role may extend beyond the Canonical Wnt Signalling Pathway. To narrow down the potential interactions and pathways in which APC participates, it would be important to further test its interactions with known partners, such as actin, myosin, and other cytoskeletal components. By examining these interactions more thoroughly, we may uncover additional functions of APC that were previously overlooked, leading to a more comprehensive understanding of its role in the remodelling of SA^{uni} neurons.

Furthermore, it has been shown that Arrow is not only a co-receptor to Frizzled in the Wnt Signalling Pathways but also operates independently of them in some contexts. This finding suggests that Arrow might play a more complex role in cellular signalling than initially realized. Given this new insight, further research should focus on investigating the mechanisms by which Arrow functions independently of the Wnt pathway. Understanding how Arrow contributes to cellular processes outside of Wnt signalling could open up new avenues for exploring its role in development.

Finally, one potential issue that could be viewed as a limitation or flaw in these experiments is the effect that the genetic manipulations might have had on the SA^{bi} neurons themselves. For example, the APC knockdown in SA^{bi} neurons resulted in the emergence of a bilateral phenotype in SAuni. This raises the possibility that the appearance or properties of the SA^{bi} neurons might have been altered in ways that influenced the phenotype of neighbouring SA^{uni} neurons. It is important to consider whether the changes observed in SA^{bi} neurons could have indirectly affected SAuni neurons, leading to the different observed phenotype in these cells.

4.6 Conclusion

In conclusion, the role of the *wnt4*^{EMS23} mutant is more intricate than initially anticipated, presenting unexpected challenges in both its characterization and the interpretation of its effects. One particularly revealing aspect of this complexity is the activation of

Armadillo in Frizzled 2-expressing glial cells in the presence of the *wnt4*^{EMS23} mutant. This observation underscores the multifaceted nature of signalling interactions and highlights the intricate crosstalk between various molecular components involved in neurodevelopment. Additionally, the discovery that APC influences cellular remodelling so strongly represents a significant breakthrough, offering new insights into the molecular underpinnings of neural development. Together, these findings illuminate the rich and interconnected network of regulatory mechanisms that govern neurodevelopmental processes. They also mark the beginning of a promising line of research aimed at unravelling how disruptions in these pathways might contribute to neurodevelopmental disorders. Continued investigation will not only deepen our understanding of fundamental developmental biology but also hold potential for informing therapeutic strategies and interventions for neurological conditions rooted in early developmental dysfunction, like epilepsy.

Literature

Abbott, J., & Näthke, I. S. (2023). The adenomatous polyposis coli protein 30 years on. *Seminars in cell & developmental biology*, *150-151*, 28–34. https://doi.org/10.1016/j.semcdb.2023.04.004

Ambesajir, A., Kaushik, A., Kaushik, J. J., & Petros, S. T. (2012). RNA interference: A futuristic tool and its therapeutic applications. *Saudi journal of biological sciences*, *19*(4), 395–403. https://doi.org/10.1016/j.sjbs.2012.08.001

Awasaki, T., Huang, Y., O'Connor, M. B., & Lee, T. (2011). Glia instruct developmental neuronal remodeling through TGF-β signaling. *Nature neuroscience*, *14*(7), 821–823. https://doi.org/10.1038/nn.2833

Bellen, H. J., Levis, R. W., He, Y., Carlson, J. W., Evans-Holm, M., Bae, E., Kim, J., Metaxakis, A., Savakis, C., Schulze, K. L., Hoskins, R. A., & Spradling, A. C. (2011). The Drosophila gene disruption project: progress using transposons with distinctive site specificities. *Genetics*, *188*(3), 731–743. https://doi.org/10.1534/genetics.111.126995

Bergmann, A., et al., 1996. A gradient of cytoplasmic Cactus degradation establishes the nuclear localization gradient of the dorsal morphogen in Drosophila. Mech. Dev. 60, 109–123. https://doi.org/10.1016/S0925-4773(96)00607-7

Brownell, H., Griffin, R., Winner, E., Friedman, O., & Happé, F. (2000). Cerebral lateralization and theory of mind. In S. Baron-Cohen, H. Tager-Flusberg, & D. J. Cohen (Eds.), *Understanding other minds: Perspectives from developmental cognitive neuroscience* (2nd ed., pp. 306–333). Oxford University Press. https://doi.org/10.1093/oso/9780198524465.003.0013

Carter Matt & Shieh Jennifer. (2015). Chapter 12 - Making and Using Transgenic Organisms. In *Guide to Research Techniques in Neuroscience* (Second Edition, pp. 253–271). Elsevier Inc. https://doi.org/10.1016/B978-0-12-800511-8.00012-5

Cooper, G. M. (2000). *The cell: a molecular approach* (2nd ed.). ASM Press; Sinauer Associates.

Coutelis, J. B., Petzoldt, A. G., Spéder, P., Suzanne, M., & Noselli, S. (2008). Left-right asymmetry in Drosophila. *Seminars in cell & developmental biology*, *19*(3), 252–262. https://doi.org/10.1016/j.semcdb.2008.01.006

Dietzl, G., Chen, D., Schnorrer, F., Su, K. C., Barinova, Y., Fellner, M., Gasser, B., Kinsey, K., Oppel, S., Scheiblauer, S., Couto, A., Marra, V., Keleman, K., & Dickson, B. J. (2007). A genome-wide transgenic RNAi library for conditional gene inactivation in Drosophila. *Nature*, *448*(7150), 151–156. https://doi.org/10.1038/nature05954

Fang, X., & Svitkina, T. M. (2022). Adenomatous Polyposis Coli (APC) in cell migration. *European journal of cell biology*, *101*(3), 151228. https://doi.org/10.1016/j.ejcb.2022.151228

Finnerty J. R. (2003). The origins of axial patterning in the metazoa: how old is bilateral symmetry?. The International journal of developmental biology, 47(7-8), 523–529.

Fradkin, L. (2023.8.15). Nrk[KO] allele. https://flybase.org/reports/FBrf0257337.html

Freeman Marc (2015). Drosophila Central Nervous System Glia. *Cold Spring Harbor perspectives in biology*, *7*(11), a020552. https://doi.org/10.1101/cshperspect.a020552

Géminard, C., González-Morales, N., Coutelis, J. B., & Noselli, S. (2014). The myosin ID pathway and left-right asymmetry in Drosophila. *Genesis (New York, N.Y. : 2000)*, *52*(6), 471–480. https://doi.org/10.1002/dvg.22763

Graba Y, Aragnol D, Rothbächer U, et al. Wnt/Wingless Signaling in Drosophila. In: Madame Curie Bioscience Database [Internet]. Austin (TX): Landes Bioscience; 2000-2013. https://www.ncbi.nlm.nih.gov/books/NBK6231/

Güntürkün, O., & Ocklenburg, S. (2017). Ontogenesis of Lateralization. *Neuron*, *94*(2), 249–263. https://doi.org/10.1016/j.neuron.2017.02.045

Hadjieconomou, D., Rotkopf, S., Alexandre, C., Bell, D. M., Dickson, B. J., & Salecker, I. (2011). Flybow: genetic multicolor cell labeling for neural circuit analysis in Drosophila melanogaster. *Nature methods*, *8*(3), 260–266. https://doi.org/10.1038/nmeth.1567

Han, JH., Kim, Y. & Cho, KO. Exosomal arrow (Arr)/lipoprotein receptor protein 6 (LRP6) in *Drosophila melanogaster* increases the extracellular level of Sol narae (Sona) in a

Wnt-independent manner. *Cell Death Dis* **11**, 944 (2020). https://doi.org/10.1038/s41419-020-02850-x

Held, Jr, L. I. (2009). SYMMETRY AND ASYMMETRY. In *Quirks of Human Anatomy: An Evo-Devo Look at the Human Body* (pp. 17–32). chapter, Cambridge: Cambridge University Press. https://doi.org/10.1017/CBO9780511626890

Hirase, H., & Shinohara, Y. (2014). Transformation of cortical and hippocampal neural circuit by environmental enrichment. *Neuroscience*, *280*, 282–298. https://doi.org/10.1016/j.neuroscience.2014.09.031

Jenett, A., Rubin, G. M., Ngo, T. T., Shepherd, D., Murphy, C., Dionne, H., Pfeiffer, B. D., Cavallaro, A., Hall, D., Jeter, J., Iyer, N., Fetter, D., Hausenfluck, J. H., Peng, H., Trautman, E. T., Svirskas, R. R., Myers, E. W., Iwinski, Z. R., Aso, Y., DePasquale, G. M., … Zugates, C. T. (2012). A GAL4-driver line resource for Drosophila neurobiology. *Cell reports*, *2*(4), 991–1001. https://doi.org/10.1016/j.celrep.2012.09.011

Joiner, D. M., Ke, J., Zhong, Z., Xu, H. E., & Williams, B. O. (2013). LRP5 and LRP6 in development and disease. *Trends in endocrinology and metabolism: TEM*, *24*(1), 31–39. https://doi.org/10.1016/j.tem.2012.10.003

Kanca, O., Zirin, J., Hu, Y., Tepe, B., Dutta, D., Lin, W. W., Ma, L., Ge, M., Zuo, Z., Liu, L. P., Levis, R. W., Perrimon, N., & Bellen, H. J. (2022). An expanded toolkit for *Drosophila* gene tagging using synthesized homology donor constructs for CRISPR-mediated homologous recombination. *eLife*, *11*, e76077. https://doi.org/10.7554/eLife.76077

Komiya, Y., & Habas, R. (2008). Wnt signal transduction pathways. *Organogenesis*, *4*(2), 68–75. https://doi.org/10.4161/org.4.2.5851

Kong, X. Z., Postema, M. C., Guadalupe, T., de Kovel, C., Boedhoe, P. S. W., Hoogman, M., Mathias, S. R., van Rooij, D., Schijven, D., Glahn, D. C., Medland, S. E., Jahanshad, N., Thomopoulos, S. I., Turner, J. A., Buitelaar, J., van Erp, T. G. M., Franke, B., Fisher, S. E., van den Heuvel, O. A., Schmaal, L., … Francks, C. (2022). Mapping brain asymmetry in health and disease through the ENIGMA consortium. *Human brain mapping*, *43*(1), 167–181. https://doi.org/10.1002/hbm.25033

Lapraz, F., Boutres, C., Fixary-Schuster, C. *et al*. Asymmetric activity of NetrinB controls laterality of the *Drosophila* brain. *Nat Commun* **14**, 1052 (2023). https://doi.org/10.1038/s41467-023-36644-4

Le Bras, A., Vijayaraj, P., & Oettgen, P. (2010). Molecular mechanisms of endothelial differentiation. *Vascular medicine (London, England)*, *15*(4), 321–331. https://doi.org/10.1177/1358863X10371685

McElwain, M. A., Ko, D. C., Gordon, M. D., Fyrst, H., Saba, J. D., & Nusse, R. (2011). A suppressor/enhancer screen in Drosophila reveals a role for wnt-mediated lipid metabolism in primordial germ cell migration. *PloS one*, *6*(11), e26993. https://doi.org/10.1371/journal.pone.0026993

Nelson, S., & Näthke, I. S. (2013). Interactions and functions of the adenomatous polyposis coli (APC) protein at a glance. *Journal of cell science*, *126*(Pt 4), 873–877. https://doi.org/10.1242/jcs.100479

Noggle, C.A., Hall, J.J. (2011). Hemispheres of the Brain, Lateralization of. In: Goldstein, S., Naglieri, J.A. (eds) Encyclopedia of Child Behavior and Development. Springer, Boston, MA. https://doi.org/10.1007/978-0-387-79061-9_1346

Pai, L. M., Orsulic, S., Bejsovec, A., & Peifer, M. (1997). Negative regulation of Armadillo, a Wingless effector in Drosophila. *Development (Cambridge, England)*, *124*(11), 2255–2266. https://doi.org/10.1242/dev.124.11.2255

Park, M., & Shen, K. (2012). WNTs in synapse formation and neuronal circuitry. *The EMBO journal*, *31*(12), 2697–2704. https://doi.org/10.1038/emboj.2012.145

Pascual, A., Huang, KL., Neveu, J. *et al.* Brain asymmetry and long-term memory. *Nature* **427**, 605–606 (2004). https://doi.org/10.1038/427605a

Perkins, L. A., Holderbaum, L., Tao, R., Hu, Y., Sopko, R., McCall, K., Yang-Zhou, D., Flockhart, I., Binari, R., Shim, H. S., Miller, A., Housden, A., Foos, M., Randkelv, S., Kelley, C., Namgyal, P., Villalta, C., Liu, L. P., Jiang, X., Huan-Huan, Q., ... Perrimon, N. (2015). The Transgenic RNAi Project at Harvard Medical School: Resources and Validation. *Genetics*, *201*(3), 843–852. https://doi.org/10.1534/genetics.115.180208

Qin, K., Yu, M., Fan, J., Wang, H., Zhao, P., Zhao, G., Zeng, W., Chen, C., Wang, Y., Wang, A., Schwartz, Z., Hong, J., Song, L., Wagstaff, W., Haydon, R. C., Luu, H. H., Ho, S. H., Strelzow, J., Reid, R. R., He, T. C., … Shi, L. L. (2023). Canonical and noncanonical Wnt signaling: Multilayered mediators, signaling mechanisms and major signaling crosstalk. *Genes & diseases*, *11*(1), 103–134. https://doi.org/10.1016/j.gendis.2023.01.030

Ripp, C., Loth, J., Petrova, I., Linnemannstöns, K., Ulepic, M., Fradkin, L., Noordermeer, J., & Wodarz, A. (2018). *Drosophila* Ror is a nervous system-specific co-receptor for Wnt ligands. *Biology open*, *7*(11), bio033001. https://doi.org/10.1242/bio.033001

Rogers L. J. (2021). Brain Lateralization and Cognitive Capacity. *Animals: an open access journal from MDPI*, *11*(7), 1996. https://doi.org/10.3390/ani11071996

Rosso, S. B., & Inestrosa, N. C. (2013). WNT signaling in neuronal maturation and synaptogenesis. *Frontiers in cellular neuroscience*, *7*, 103. https://doi.org/10.3389/fncel.2013.00103

R Core Team (2021). R: A language and environment for statistical computing. R Foundation for Statistical Computing, Vienna, Austria. URL https://www.R-project.org/.

Scheffer, L. K., Xu, C. S., Januszewski, M., Lu, Z., Takemura, S. Y., Hayworth, K. J., Huang, G. B., Shinomiya, K., Maitlin-Shepard, J., Berg, S., Clements, J., Hubbard, P. M., Katz, W. T., Umayam, L., Zhao, T., Ackerman, D., Blakely, T., Bogovic, J., Dolafi, T., Kainmueller, D., … Plaza, S. M. (2020). A connectome and analysis of the adult *Drosophila* central brain. *eLife*, *9*, e57443. https://doi.org/10.7554/eLife.57443

Schindelin, J., Arganda-Carreras, I., Frise, E., Kaynig, V., Longair, M., Pietzsch, T., Preibisch, S., Rueden, C., Saalfeld, S., Schmid, B., Tinevez, J. Y., White, D. J., Hartenstein, V., Eliceiri, K., Tomancak, P., & Cardona, A. (2012). Fiji: an open-source platform for biological-image analysis. *Nature methods*, *9*(7), 676–682. https://doi.org/10.1038/nmeth.2019

Schnorrer, F., & Dickson, B. J. (2004). Axon guidance: morphogens show the way. *Current biology: CB*, *14*(1), R19–R21. https://doi.org/10.1016/j.cub.2003.12.016

Sivasankaran, R., Calleja, M., Morata, G., & Basler, K. (2000). The Wingless target gene Dfz3 encodes a new member of the Drosophila Frizzled family. *Mechanisms of development*, *91*(1-2), 427–431. https://doi.org/10.1016/s0925-4773(99)00313-5

Sun, H., Shah, A. S., Bonfini, A., Buchon, N. S., & Baskin, J. M. (2023). Wnt/β-catenin signaling within multiple cell types dependent upon *kramer* regulates *Drosophila* intestinal stem cell proliferation. *bioRxiv : the preprint server for biology*, 2023.02.21.529411. https://doi.org/10.1101/2023.02.21.529411

Takagi, Suguru & Takano, Shiina & Hashimoto, Yusaku & Morise, Shu & Zeng, Xiangsunze & Nose, Akinao. (2024). Segment-specific axon guidance by Wnt/Fz signaling diversifies motor commands in Drosophila larvae. *eLife***13**:RP98624. https://doi.org/10.7554/eLife.98624.1

Tamai, K., Zeng, X., Liu, C., Zhang, X., Harada, Y., Chang, Z., & He, X. (2004). A mechanism for Wnt coreceptor activation. *Molecular cell*, *13*(1), 149–156. https://doi.org/10.1016/s1097-2765(03)00484-2

Tearle, R.G., Nusslein-Volhard, C. (1987). Tubingen mutants and stock list. D. I. S. 66(): 209--269.

Tolwinski N. S. (2017). Introduction: Drosophila-A Model System for Developmental Biology. *Journal of developmental biology*, *5*(3), 9. https://doi.org/10.3390/jdb5030009

Turrigiano G. G. (1999). Homeostatic plasticity in neuronal networks: the more things change, the more they stay the same. *Trends in neurosciences*, *22*(5), 221–227. https://doi.org/10.1016/s0166-2236(98)01341-1

Upadhyay, A., Moss-Taylor, L., Kim, M. J., Ghosh, A. C., & O'Connor, M. B. (2017). TGF-β Family Signaling in *Drosophila*. *Cold Spring Harbor perspectives in biology*, *9*(9), a022152. https://doi.org/10.1101/cshperspect.a022152

Wehrli, M., Dougan, S. T., Caldwell, K., O'Keefe, L., Schwartz, S., Vaizel-Ohayon, D., Schejter, E., Tomlinson, A., & DiNardo, S. (2000). arrow encodes an LDL-receptor-related protein essential for Wingless signalling. *Nature*, *407*(6803), 527–530. https://doi.org/10.1038/35035110

Wolff, T., & Rubin, G. M. (2018). Neuroarchitecture of the Drosophila central complex: A catalog of nodulus and asymmetrical body neurons and a revision of the protocerebral bridge catalog. *The Journal of comparative neurology*, *526*(16), 2585–2611. https://doi.org/10.1002/cne.24512

Won, J. H., Kim, G. W., Kim, J. Y., Cho, D. G., Kwon, B., Bae, Y. K., & Cho, K. O. (2019). ADAMTS Sol narae cleaves extracellular Wingless to generate a novel active form that regulates cell proliferation in Drosophila. *Cell death & disease*, *10*(8), 564. https://doi.org/10.1038/s41419-019-1794-8

Wu, J., Roman, A. C., Carvajal-Gonzalez, J. M., & Mlodzik, M. (2013). Wg and Wnt4 provide long-range directional input to planar cell polarity orientation in Drosophila. *Nature cell biology*, *15*(9), 1045–1055. https://doi.org/10.1038/ncb2806

Zhou, C. J., Zhao, C., & Pleasure, S. J. (2004). Wnt signaling mutants have decreased dentate granule cell production and radial glial scaffolding abnormalities. *The Journal of neuroscience: the official journal of the Society for Neuroscience*, *24*(1), 121–126. https://doi.org/10.1523/JNEUROSCI.4071-03.2004